NASA TECHNICAL NOTE

NASA TN D-4182

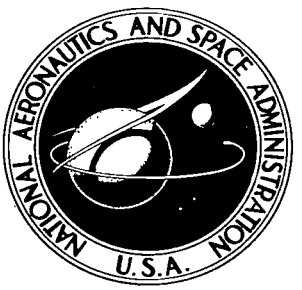

STATIC AERODYNAMIC CHARACTERISTICS OF THREE RAM-AIR-INFLATED LOW-ASPECT-RATIO FABRIC WINGS

by Sanger M. Burk, Jr., and George M. Ware

Langley Research Center
Langley Station, Hampton, Va.

NATIONAL AERONAUTICS AND SPACE ADMINISTRATION • WASHINGTON, D. C. • SEPTEMBER 1967

NASA TN D-4182

STATIC AERODYNAMIC CHARACTERISTICS OF THREE RAM-AIR-INFLATED LOW-ASPECT-RATIO FABRIC WINGS

By Sanger M. Burk, Jr., and George M. Ware

Langley Research Center
Langley Station, Hampton, Va.

NATIONAL AERONAUTICS AND SPACE ADMINISTRATION

For sale by the Clearinghouse for Federal Scientific and Technical Information
Springfield, Virginia 22151 – CFSTI price $3.00

STATIC AERODYNAMIC CHARACTERISTICS OF THREE RAM-AIR-INFLATED LOW-ASPECT-RATIO FABRIC WINGS

By Sanger M. Burk, Jr., and George M. Ware
Langley Research Center

SUMMARY

An investigation of the low-speed static aerodynamic characteristics of three ram-air-inflated low-aspect-ratio fabric wings has been made in the Langley full-scale tunnel. The wings which were rectangular in planform and had an airfoil-shaped cross section were open at the nose to allow air to enter and inflate the wings; the payload was suspended on lines below the wings. Effects of four different test setups were also determined.

The results indicated that the untrimmed maximum lift-drag ratios of the wings ranged from 1.9 to 2.7 and that the untrimmed maximum lift coefficients varied from about 0.9 to 1.1. The results of tests of two of the wings selected for a study of their stability characteristics indicated that they were statically longitudinally stable over the entire test angle-of-attack range of 0^{o} to 70^{o} except for a slight unstable break in the pitching-moment curves at angles of attack just beyond that for the stall. Both of these wings had generally satisfactory static lateral stability characteristics over the entire test angle-of-attack range.

INTRODUCTION

There is, at the present time, an increasing interest in gliding parachutes as a means of space vehicle recovery and cargo delivery, and there are a number of different types of gliding parachutes being developed to meet the demand for such a system. In order to evaluate the performance, stability and control, and deployment characteristics of such configurations, the Langley Research Center is presently evaluating several parachute-like devices with gliding capability by means of wind-tunnel and flight tests.

One concept in the gliding-parachute category which has received attention is a ram-air-inflated fabric wing (called the Jalbert Parafoil). It has a rectangular planform and an airfoil cross section with an opening at the leading edge to allow ram air to enter and inflate the wing to the desired shape. The payload is suspended on lines below the wing. The results of some preliminary wind-tunnel tests and free-flight tests on this type of wing are presented in reference 1.

The purpose of the present investigation is to provide some basic information on the static longitudinal and lateral aerodynamic characteristics of this type of ram-air-inflated wing. Three wings which varied somewhat in aspect ratio, thickness ratio, and inlet design were tested in the Langley full-scale tunnel. The original model (wing I) was procured from the manufacturer and the other two models (wings II and III) were refined configurations made available for testing by the University of Notre Dame. The tests, using several different techniques, were made over an angle-of-attack range from as low as 0° to as high as 90° and over a sideslip range from 10° to -10°.

SYMBOLS

The longitudinal and lateral data are referred to the wind and body system of axes, respectively, which are shown in figure 1. The moment reference center was located 4.0 percent of the wing chord aft of the most forward portion of the leading edge of the wing and 123.0 percent of the wing chord below the lower surface of the wing. The units used for the physical quantities defined in this paper are given both in the U.S. Customary Units and in the International System of Units (SI). Factors relating the two systems are given in reference 2.

b	wing span, ft (m)
c	wing chord, ft (m)
C_D	drag coefficient, $\frac{\text{Drag}}{qS}$
C_L	lift coefficient, $\frac{\text{Lift}}{qS}$
C_l	rolling-moment coefficient, $\frac{\text{Rolling moment}}{qSb}$
C_{l_β}	effective-dihedral parameter, $\frac{\partial C_l}{\partial \beta}$, per deg
C_m	pitching-moment coefficient, $\frac{\text{Pitching moment}}{qSc}$
C_n	yawing-moment coefficient, $\frac{\text{Yawing moment}}{qSb}$
C_{n_β}	directional-stability parameter, $\frac{\partial C_n}{\partial \beta}$, per deg
C_Y	side-force coefficient, $\frac{\text{Side force}}{qS}$

C_{Y_β}	side-force parameter, $\frac{\partial C_Y}{\partial \beta}$, per deg
L/D	lift-drag ratio
q	free-stream dynamic pressure, $\frac{\rho V^2}{2}$, lb/ft^2 (N/m^2)
S	wing area, ft^2 (m^2)
V	airspeed, ft/sec (m/s)
X,Y,Z	coordinate axes
α	angle of attack, deg
β	angle of sideslip, deg
ρ	air density, slugs/ft^3 (kg/m^3)

Subscript:

max	maximum value

MODELS

Sketches of the wings which are referred to as wings I, II, and III are presented in figures 2, 3, and 4; the physical characteristics of the wings are presented in table I. The wings were made of approximately 1.1 oz/yd^2 (0.0373 kg/m^2) low-porosity acrylic-coated nylon. The three wings were rectangular in planform and had airfoil sections with flat undersurfaces. The leading edges of the wings were open to allow ram air to enter and inflate the wing. The shape of the wing was determined by fabric ribs which were constructed into the wing at approximately evenly spaced distances along the span. Very small vents or exhaust ports were located at the trailing edges of the wings between the ribs. The payload was supported below the wings by nylon suspension lines. The wings, in general, had triangular fabric panels on the undersurface for the purpose of distributing the suspension line loads evenly to the wing.

TABLE I.- DIMENSIONAL CHARACTERISTICS

Wing dimensions	Wing I	Wing II	Wing III
Span, ft (m)	4.50 (1.37)	4.50 (1.37)	6.13 (1.87)
Chord, ft (m)	7.04 (2.15)	5.79 (1.77)	6.56 (2.00)
Area, ft^2 (m^2)	31.69 (2.95)	26.05 (2.42)	40.21 (3.74)
Aspect ratio	0.64	0.78	0.94
Thickness ratio	0.201	0.126	0.184
Inlet opening angle measured from horizontal, deg	18	42	45

Capsule dimensions	
Maximum diameter, ft (m)	1.11 (0.34)
Minimum diameter, ft (m)	0.58 (0.18)
Height, ft (m)	0.58 (0.18)

APPARATUS AND TESTING TECHNIQUE

The models were tested in the Langley full-scale tunnel, a complete description of which is given in reference 3. The forces and moments acting on the wings were measured by an externally mounted six-component strain-gage balance.

Four test setups were used during the investigation in an effort to determine a method of supporting the wings in the desired test attitude that would not overly compromise the characteristics of the fabric wings by the restraint imposed by the support system. These test setups are described in the following paragraphs. For a comparison of techniques, wing II was tested with each of the four test setups. Wing I was tested only with setup 1, and wing III was tested only with setup 3.

Test Setup 1

The first test setup used in the investigation is illustrated in figures 5 and 6. In this setup, the confluence point of the wing suspension lines was attached to a beam that had its major axis parallel to the wing chord. The beam, in turn, was secured to a strain-gage balance. In order to restrain the wing so that the pitching moment could be measured, the wing was also held by single lines attached at the nose and trailing edge extending downward and outward to the beam. As the angle of attack of the beam was changed, the wing would follow. However, there was some difference in the angle of attack of the beam and the wing because of model deformation and translation of the wing

fore and aft on the lines. This angle-of-attack difference was measured from film records of the force tests and taken into account in the presentation of the data. Because of the translation of wing, it was difficult to determine the exact position of the wing relative to the moment center of the strain-gage balance. As a result, large errors were introduced into the pitching-moment data and thus these data are not presented.

Test Setup 2

The second test setup is illustrated in figures 7 and 8. For this test setup a tubular gridwork was substituted for the beam of setup 1 and the leading- and trailing-edge restraint lines were removed. The model suspension lines were shortened by about one-half their length and attached at their intersection with the grid. This procedure resulted in a model suspension-line configuration above the gridwork which was about the same as that of setup 1. This type of mounting restrained the wing somewhat in both the longitudinal and lateral planes. Again, as in test setup 1, there was some deformation and some translation of the wing. The lift and drag data were corrected for this difference but the pitching-moment data, for the reason previously discussed, was felt to be in error and are not presented.

Test Setup 3

A sketch of the third test setup is shown in figure 9 and photographs are presented in figure 10. In this setup a spine consisting of metal angles placed back to back was attached to the underside of the wing along its center line and a tubular metal boom extending downward from the spine formed an anchor point for the model suspension lines. The system was then mounted on the strain-gage balance. With the wing held firmly by this method, there was no change in the position of the wing with respect to the balance due to changes in angle of attack or angles of sideslip. All static longitudinal and lateral coefficients of the model were determined for this technique and are presented.

In order to determine the effect of a payload on the aerodynamic characteristics of one of the wings, an Apollo-type capsule was added to wing III, as shown in figure 11, for some brief tests.

Test Setup 4

Test setup 4 is illustrated in figure 12. In this case, the suspension lines of the wing were attached very closely together on a small bracket attached to the strain-gage balance, and the wing was allowed to fly freely. A lateral oscillation of the wing developed in this free-flying condition, and it was necessary to restrain the wing laterally by means of light lines extending spanwise perpendicular to the wing chord plane. Although

these lines were not instrumented, it was felt that the forces and moments contributed by the lines were small. For this test setup, the angle of attack of the model was changed by adjusting the suspension-line lengths. In adjusting the suspension lines, an attempt was made to maintain a constant flat-bottomed airfoil shape.

TESTS

Force tests were made over an angle-of-attack range from as low as 0° to as high as 90° to determine the static longitudinal stability characteristics of the wings. Data for angles of attack below 10° were impossible to obtain with test setups 1 and 2, which gave the models the least lateral restraint of the test methods, because the wing diverged directionally. At angles of attack above about 70° regardless of which test setup was used, the wings would not inflate properly and the model became deformed. Motion-picture records of all test conditions were made for more detailed study of configuration shape and for use in determining the wing angle of attack in test setups 1, 2, and 4. The static lateral stability characteristics, which could only be obtained with the rigid-spine test setup, were measured over an angle-of-sideslip range from 10° to -10° for angles of attack from 0° to 70°. The dynamic pressure used in the investigation was varied from about 0.50 to 1.50 lb/ft^2 (23.9 to 71.8 N/m^2), which corresponded to an airspeed range from about 20 to 40 ft/sec (6.1 to 12.2 m/s) at standard sea-level conditions and a Reynolds number range from about 127,000 to 255,000 per unit length. No corrections were made to the data for the aerodynamic tares of the support systems.

RESULTS AND DISCUSSION

Longitudinal Characteristics

The results of the tests to determine the longitudinal characteristics are presented in figures 13 to 16 and a comparison of the values of maximum lift coefficient and maximum lift-drag ratio for the wings as tested on the various setups are presented in table II. Unless otherwise noted, the maximum lift-coefficient and lift-drag-ratio values discussed are for untrimmed conditions.

Comparison of testing technique.- The lift, drag, and lift-drag-ratio characteristics of wing II as determined with test setups 1, 2, and 3 (beam, gridwork, and rigid spine methods, respectively) are compared with the results for test setup 4 (tethered method) in figure 13. The results showed that the maximum lift coefficient of the wing occurred at approximately the same angle of attack (30° to 35°) regardless of the test setup used, but that there was a considerable difference in the magnitude of $C_{L_{max}}$

TABLE II.- COMPARISON OF MAXIMUM LIFT COEFFICIENT AND LIFT-DRAG RATIOS OF VARIOUS WING CONFIGURATIONS FOR VARIOUS TEST SETUPS

Test setup	Tunnel velocity, ft/sec (m/s)	$C_{L_{max}}$	$(L/D)_{max}$
	Wing I		
1	20 (6.1)	0.98	1.9
	Wing II		
1	20 (6.1)	1.32	2.25
2	20 (6.1)	1.12	2.30
3	20 (6.1)	1.02	2.40
3	40 (12.2)	1.11	2.55
4	20 (6.1)	1.02	2.30
	Wing III		
3	20 (6.1)	0.92	2.70
3	30 (9.1)	.88	2.60
3 (wing plus capsule)	30 (9.1)	.88	2.55

(ranging from 1.02 to 1.32) as determined with the various test setups. The data obtained with the rigid-spine setup fairly closely approximated the data of the tethered tests. The relatively large differences in data for test setups 1 and 2, particularly in maximum lift coefficient, were believed to have been the result of increased camber of the wing caused by the method of model restraint. (See fig. 6.) The rigid-spine technique, of course, held the model in a flat-bottomed configuration, and during the tethered tests the suspension lines of the model were adjusted to give a flat-bottomed airfoil shape which is the shape of the wing as determined from brief free gliding tests of the model. To permit testing over the entire range of test conditions of interest, however, the wing must have more restraint than is provided by setup 4. In particular, it is necessary to restrain the wing in order to determine its static longitudinal, lateral, and directional stability and to prevent violent oscillations at high angles of attack (angles above about 50^{o}). These oscillations do not necessarily indicate dynamic instability in free flight, but are characteristic of gliding parachutes at high angles of attack when the device is restrained at the confluence of the suspension lines for wind-tunnel tests. As a result of these considerations, most of the tests were conducted with setup 3.

Wing I.- The aerodynamic characteristics of wing I, which were determined only with test setup 1, are presented in figure 14. It was noted from visual observations of

the tests that the upper surface of the wing had a tendency to buckle upward at about the quarter-chord line and to develop large wrinkles forward of this point. (See fig. 6.) As a result of this distortion, the performance of the model suffered and the maximum lift-drag ratio was only 1.9. Because of the deformation and relatively low value of the lift-drag ratio, no further tests were made with wing I.

Wing II.- The four testing techniques, as previously mentioned, were used in determining the longitudinal aerodynamic characteristics of wing II. The characteristics of the wing were more extensively examined by the rigid-spine technique and these data are presented in figures 15(a) and 16. The results indicated that the wing was statically longitudinally stable at angles of attack up to those just beyond the stall where a slight unstable break in the pitching-moment curve occurred. At still higher angles of attack the wing became stable again. The model was in trim at an angle of attack of about 5^{o} which is very nearly the angle for the maximum value of lift-drag ratio. The data of figure 15(a) indicate that airspeed could have an appreciable effect on the aerodynamic characteristics of the wing. For example, at the lower speed (20 ft/sec or 6.1 m/s), the value of maximum lift was 1.02, whereas with an airspeed of 40 ft/sec (12.2 m/s) the maximum lift coefficient was increased to 1.11. There was also an increase in maximum lift-drag ratio from 2.45 to 2.55 and an increase in longitudinal stability. The increase in lift with increasing airspeed is believed to be caused mainly by changes in the shape of the wing due to aerodynamic loading.

Wing III.- The longitudinal aerodynamic characteristics of wing III as tested with setup 3 (rigid spine) are presented in figure 15(b). These tests were made at airspeeds of 20 ft/sec (6.1 m/s) and 30 ft/sec (9.1 m/s). An attempt was made to conduct the tests at 40 ft/sec (12.2 m/s), but the wing was deformed so badly that it was decided not to test at this speed. There is a possibility that there was some minor deformation at the 30 ft/sec (9.1 m/s) condition, but from visual observation the wing appeared to be well formed. For one test a small model of an Apollo-type spacecraft was added to the configuration (see fig. 11) in order to determine the effect that a payload might have on the aerodynamic characteristics of the model. The data indicate that there was very little effect on the characteristics of the model due either to the change in airspeed or to the addition of the payload.

A comparison of the aerodynamic characteristics of wing III with those of wing II is shown in figure 16. These data indicate that wing III had a somewhat higher $(L/D)_{max}$ than wing II. This result was due mainly to lower values of drag coefficient since wing III had a lower lift-curve slope and a lower maximum lift coefficient than wing II.

Lateral Characteristics

The static lateral aerodynamic characteristics of wing II and wing III when using test setup 3 were determined, in general, over an angle-of-attack range from 5° to 60° for a sideslip range up to $\pm 10^{\circ}$. The results of these tests are presented in figure 17 and summarized in figure 18 in the form of the stability derivatives C_{Y_β}, C_{n_β}, and C_{l_β} plotted against angle of attack. The values of these derivatives were obtained from the differences between the values of the coefficients measured at sideslip angles of 5° and -5°.

In general, the variation of the lateral coefficients of the wings with angle of sideslip was fairly linear. (See fig. 17.) The data presented in figure 18 show that all the wings had positive effective dihedral $\left(-C_{l_\beta}\right)$ and positive directional stability $\left(C_{n_\beta}\right)$ over the entire angle-of-attack range. There was a large increase in the values of these parameters as the stall angle of attack was approached and then a fairly rapid decrease.

SUMMARY OF RESULTS

The results of an investigation in the Langley full-scale tunnel to determine the static aerodynamic characteristics of three ram-air-inflated low-aspect-ratio fabric wings may be summarized as follows:

1. The untrimmed maximum lift-drag ratios of the three wings ranged from 1.9 to 2.7 and the untrimmed maximum lift coefficients varied from about 0.9 to 1.1.

2. Two of the wings selected for a study of their static stability characteristics were longitudinally stable over the entire angle-of-attack range from 0° to 70°, except for a slight destabilizing break in the pitching-moment curves at angles of attack just above that for the stall, and both of these wings had generally satisfactory static lateral stability characteristics over the entire angle-of-attack range.

Langley Research Center,
National Aeronautics and Space Administration,
Langley Station, Hampton, Va., June 15, 1967,
124-07-03-06-23.

REFERENCES

1. Nicolaides, John D.; and Knapp, Charles F.: A Preliminary Study of the Aerodynamics and Flight Performance of the Parafoil. Dept. Aerospace Eng., Univ. Notre Dame, July 1965.

2. Mechtly, E. A.: The International System of Units – Physical Constants and Conversion Factors. NASA SP-7012, 1964.

3. DeFrance, Smith J.: The N.A.C.A. Full-Scale Wind Tunnel. NACA Rept. 459, 1933.

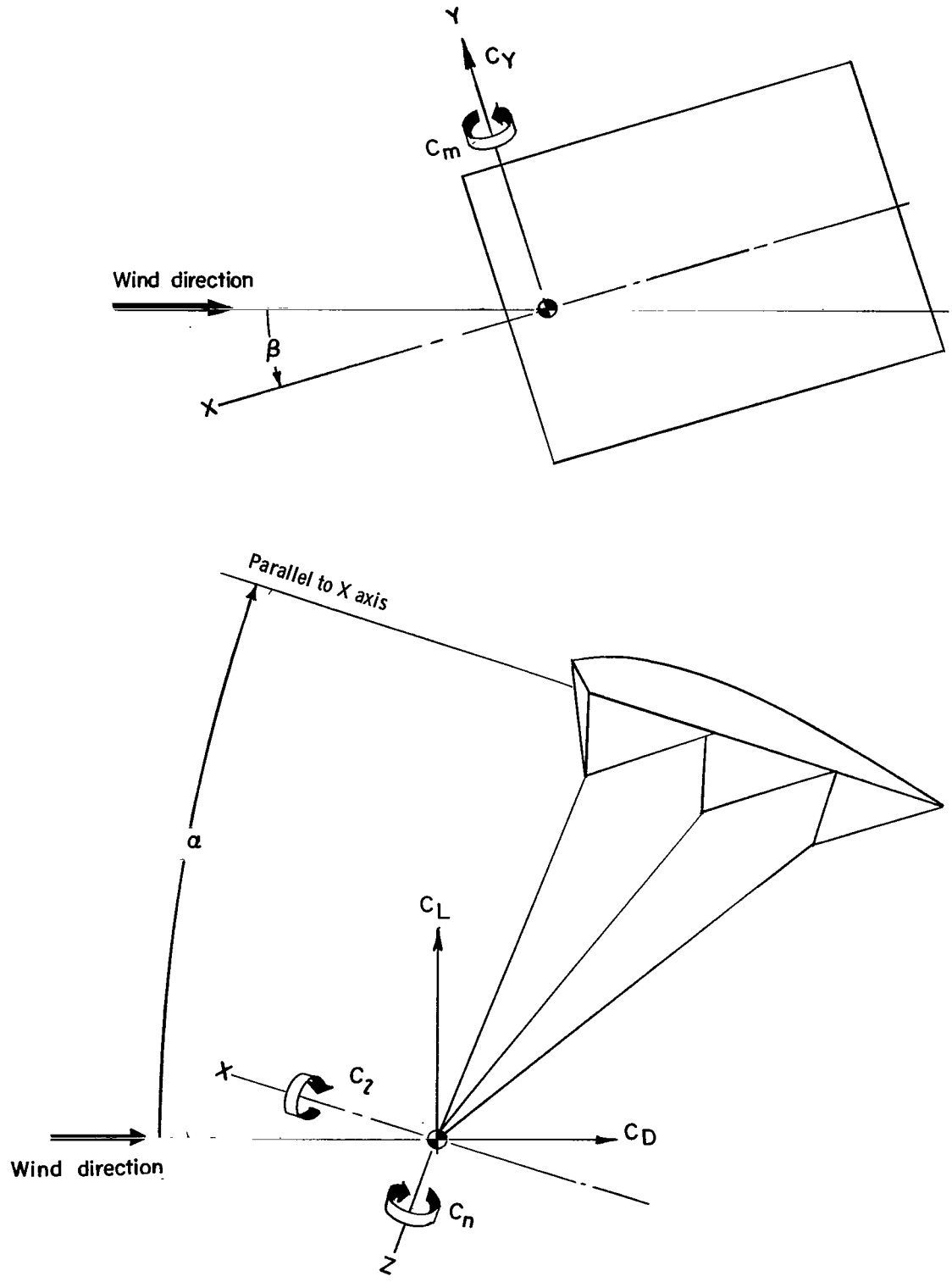

Figure 1.- System of axes used in the investigation. Longitudinal data are referred to wind axes and lateral data are referred to body axes. Arrows indicate positive direction of moments, forces, and angles.

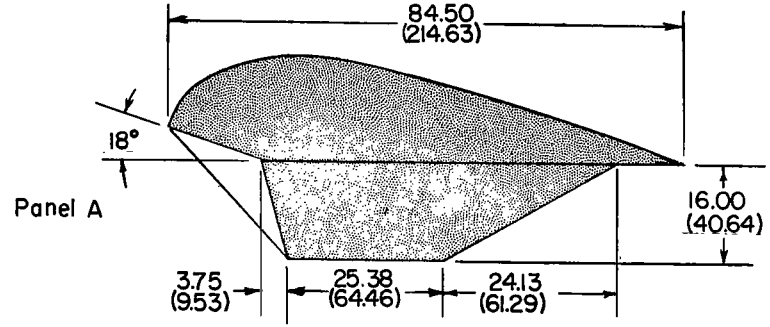

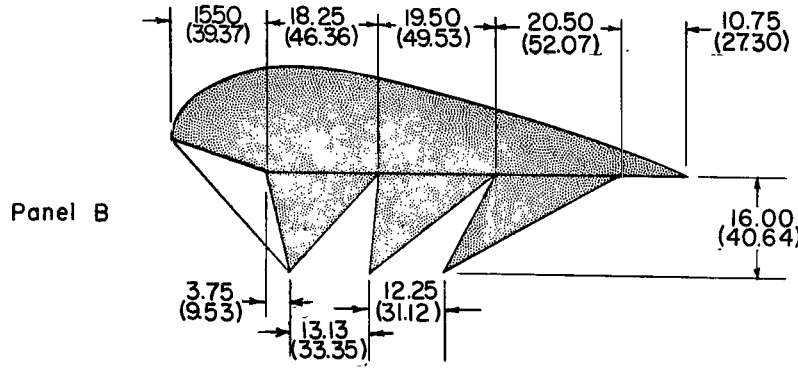

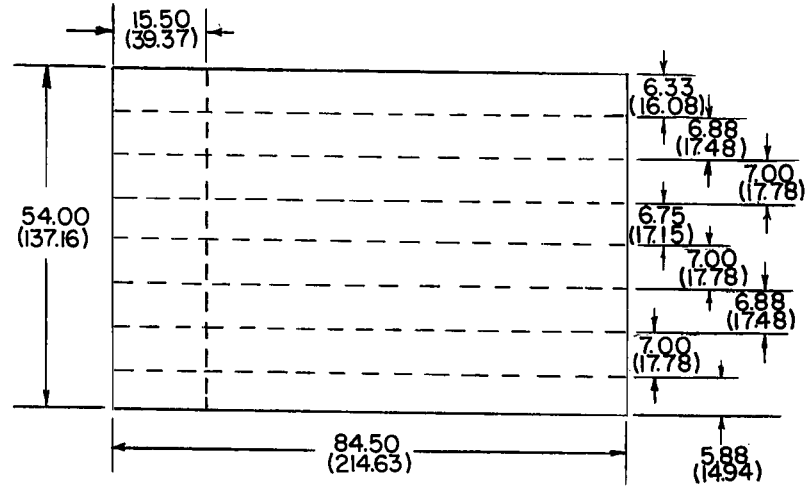

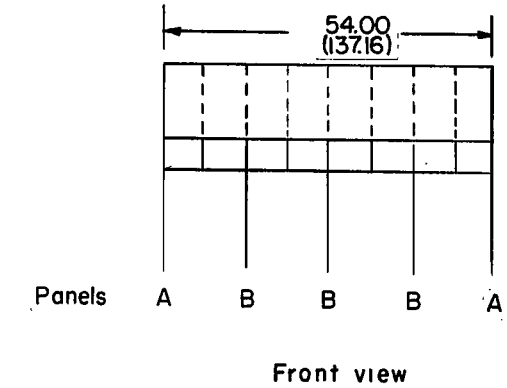

Airfoil ordinates
(Stations and ordinates given in percent of airfoil chord)

Upper surface	
Station	Ordinate
0.00	6.065
1.25	8.875
2.50	10.947
5.00	13.314
7.50	15.385
10.00	16.420
15.00	18.047
20.00	19.527
25.00	20.118
30.00	19.527
40.00	18.047
50.00	15.385
60.00	13.166
70.00	10.651
80.00	7.396
90.00	3.846
100.00	0.000

Figure 2.- Geometry of wing 1. For clarity some views are shaded. Initial dimensions are in inches; parenthetical dimensions are in centimeters.

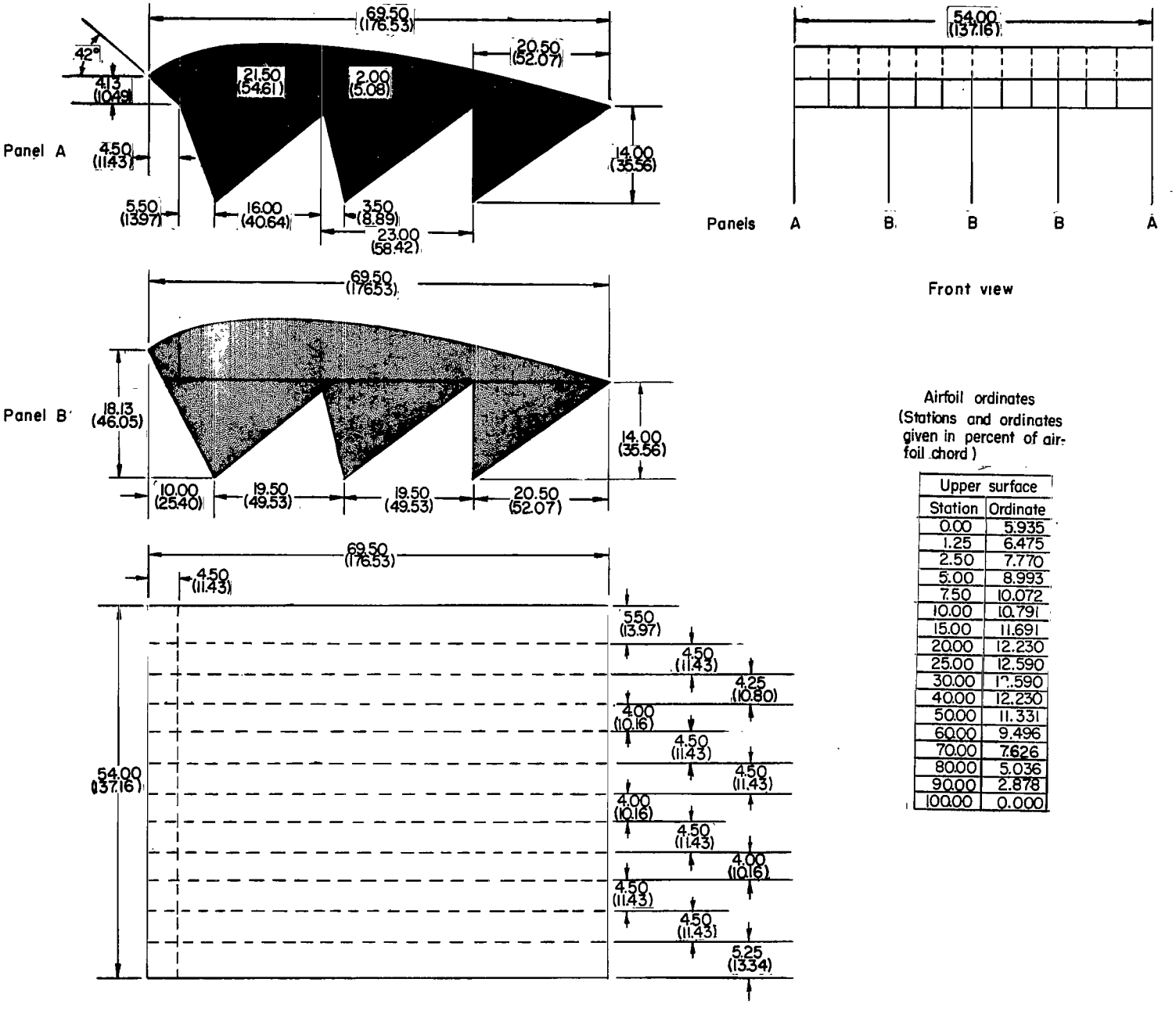

Airfoil ordinates
(Stations and ordinates given in percent of airfoil chord)

Upper surface	
Station	Ordinate
0.00	5.935
1.25	6.475
2.50	7.770
5.00	8.993
7.50	10.072
10.00	10.791
15.00	11.691
20.00	12.230
25.00	12.590
30.00	12.590
40.00	12.230
50.00	11.331
60.00	9.496
70.00	7.626
80.00	5.036
90.00	2.878
100.00	0.000

Figure 3.- Geometry of wing 11. For clarity some views are shaded. Initial dimensions are in inches; parenthetical dimensions are in centimeters.

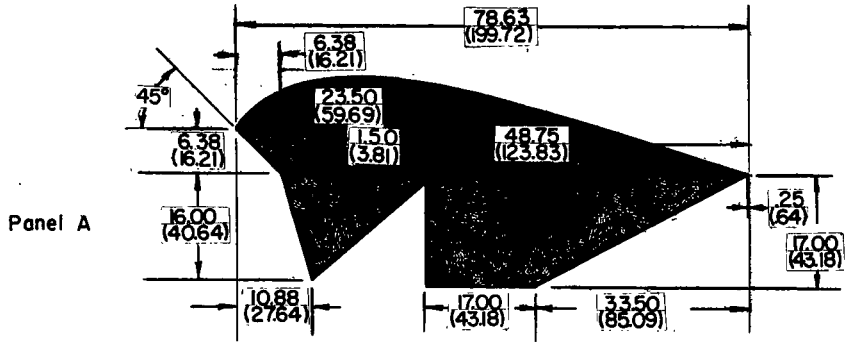

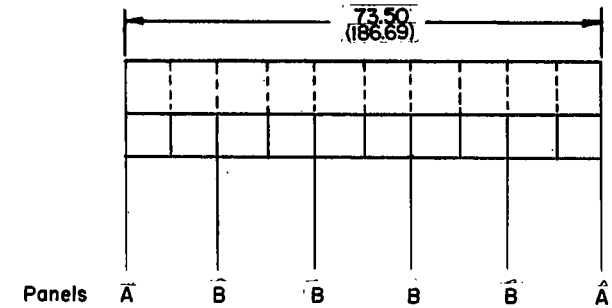

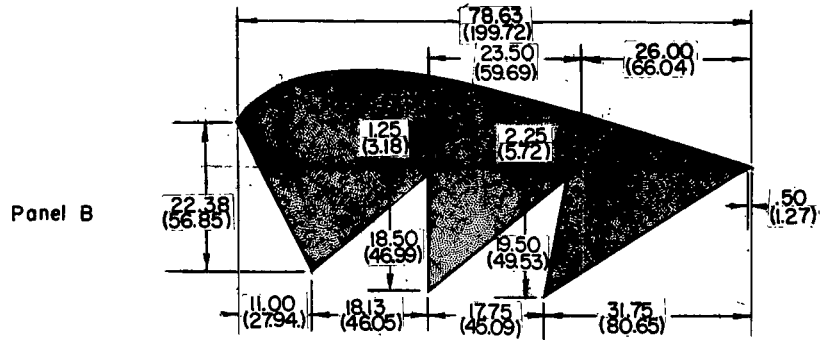

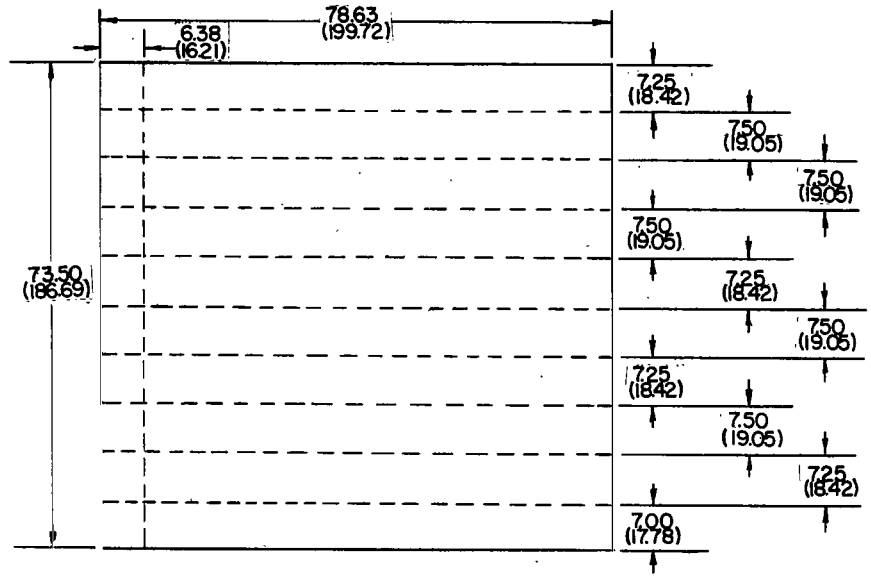

Airfoil ordinates

(Station and ordinates given in percent of airfoil chord)

Upper surface	
Station	Ordinate
0.00	8.108
1.25	10.811
2.50	12.083
5.00	13.990
7.00	15.262
10.00	16.216
15.00	17.488
20.00	18.124
25.00	18.442
30.00	18.124
40.00	16.534
50.00	14.372
60.00	12.083
70.00	9.157
80.00	6.041
90.00	2.862
100.00	0.000

Figure 4.- Geometry of wing III. For clarity some views are shaded. Initial dimensions are in inches; parenthetical dimensions are in centimeters.

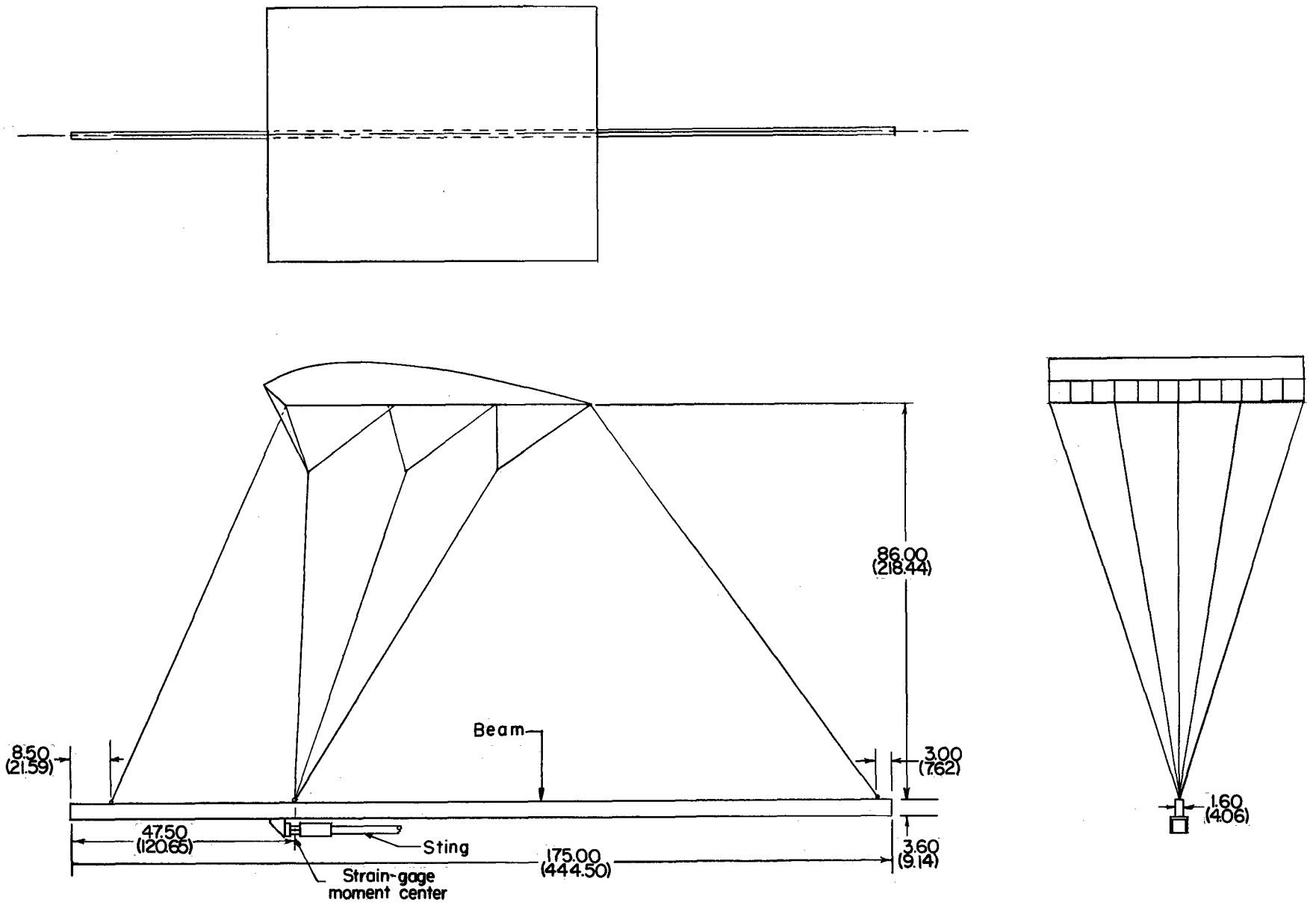

Figure 5.- Sketch of model mounted on test setup 1. Initial dimensions are in inches; parenthetical dimensions are in centimeters. For clarity some hidden lines are omitted in figure.

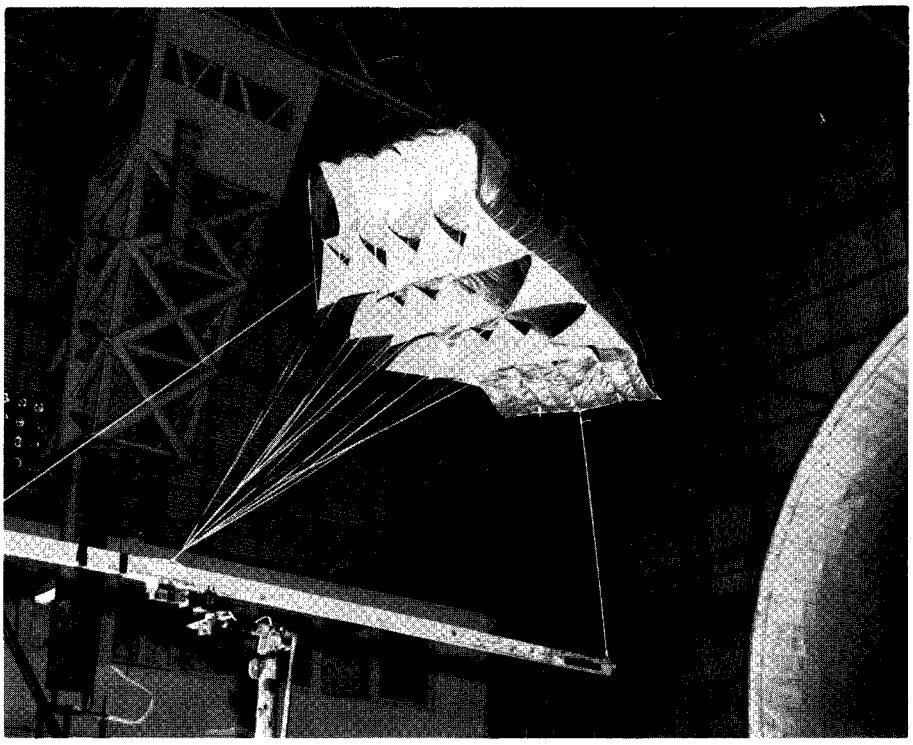

L-65-2172

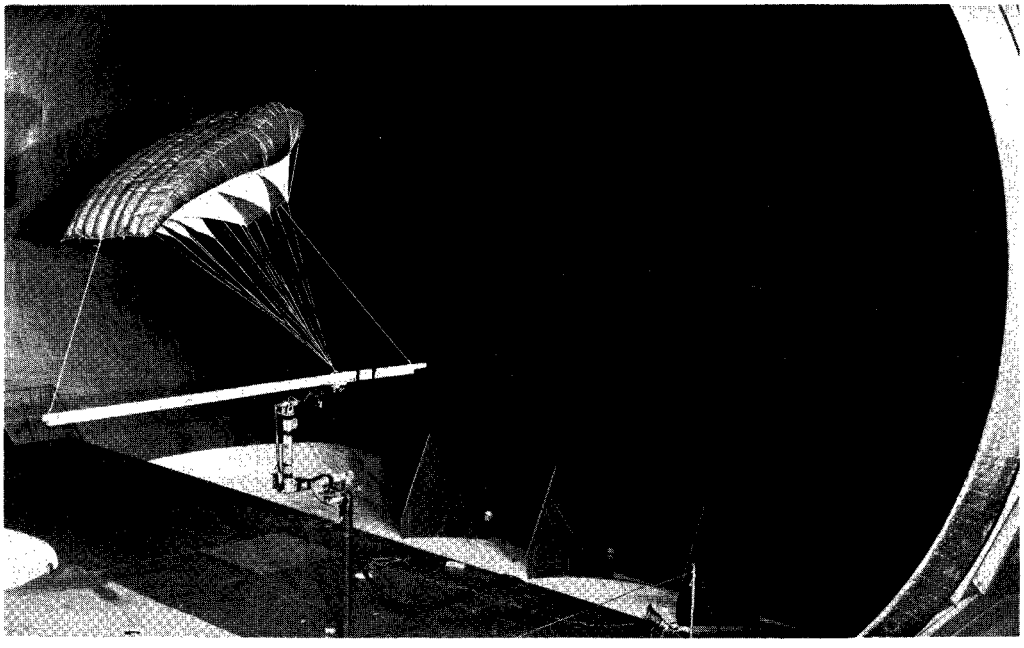

(a) Wing I; test setup 1. L-65-2170

Figure 6.- Wings I and II mounted on test setup 1 in Langley full-scale tunnel.

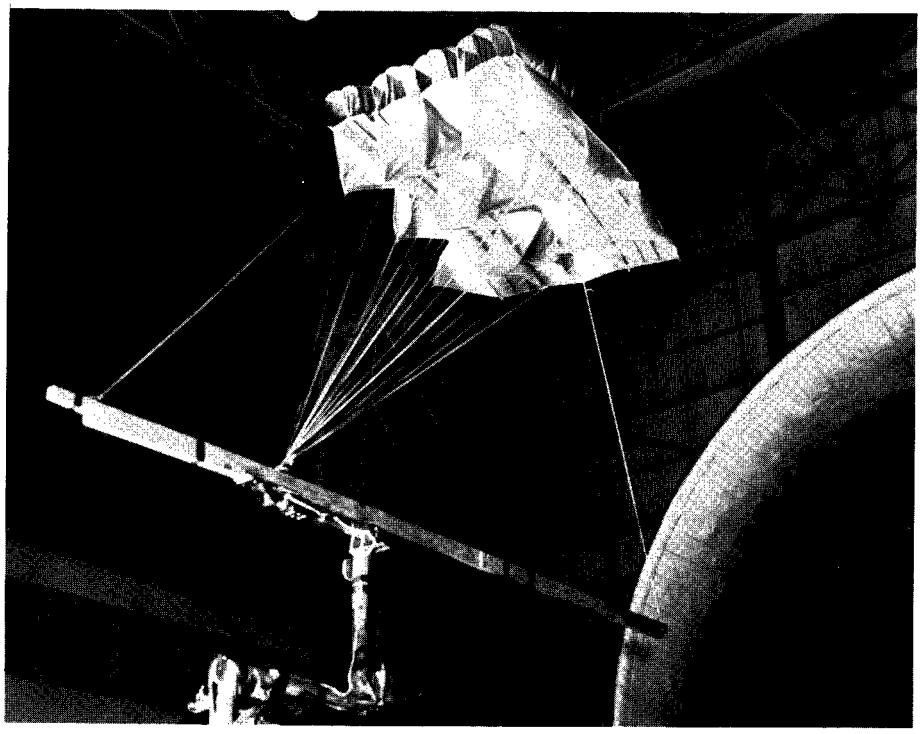

L-65-2715

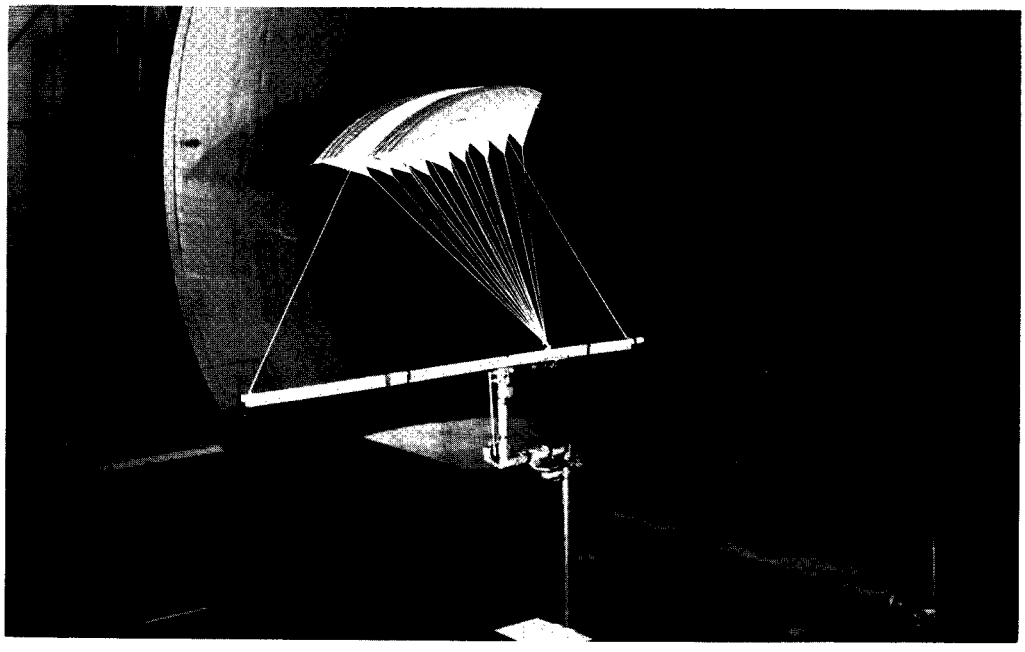

(b) Wing II; test setup 1. L-65-2717

Figure 6.- Concluded.

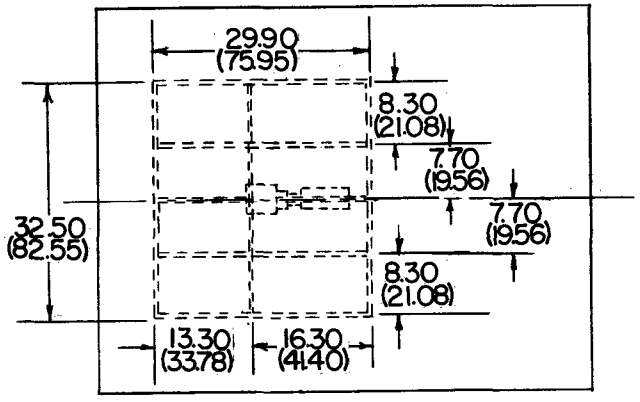

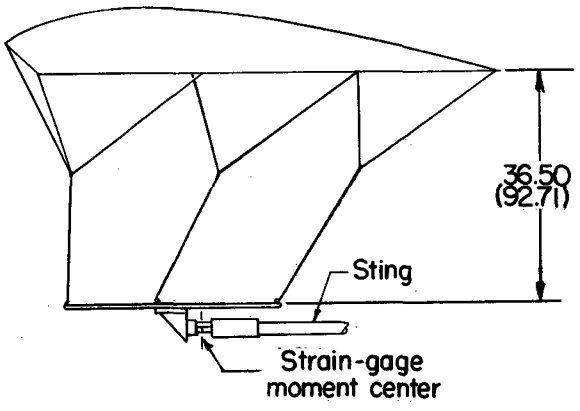

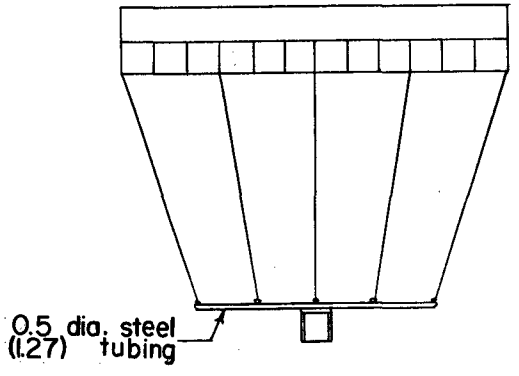

Figure 7.- Sketch of model mounted on test setup 2. Initial dimensions are in inches; parenthetical dimensions are in centimeters. For clarity some hidden lines are omitted in figure.

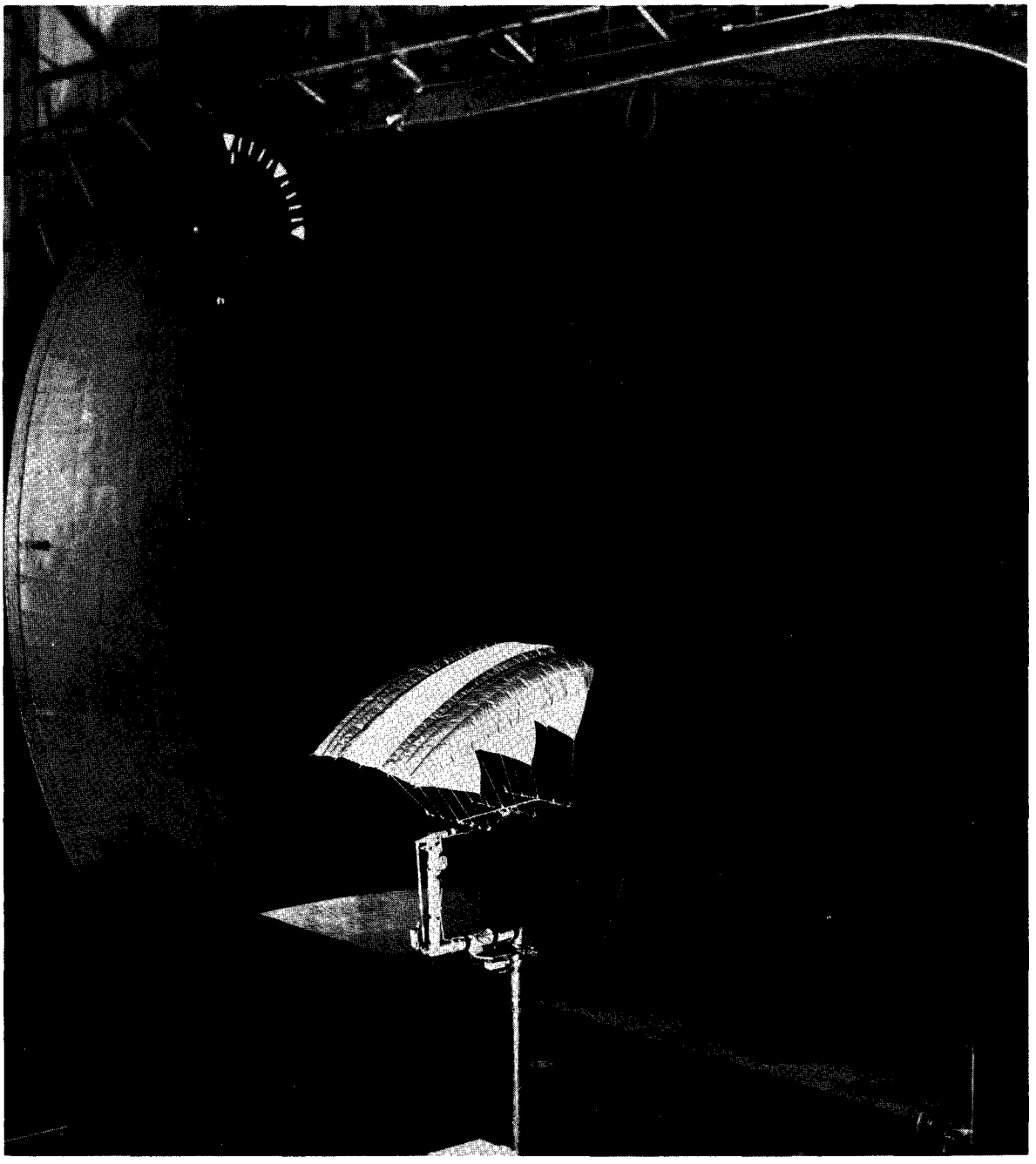

Figure 8.- Wing II mounted on test setup 2 in Langley full-scale tunnel. L-65-2719

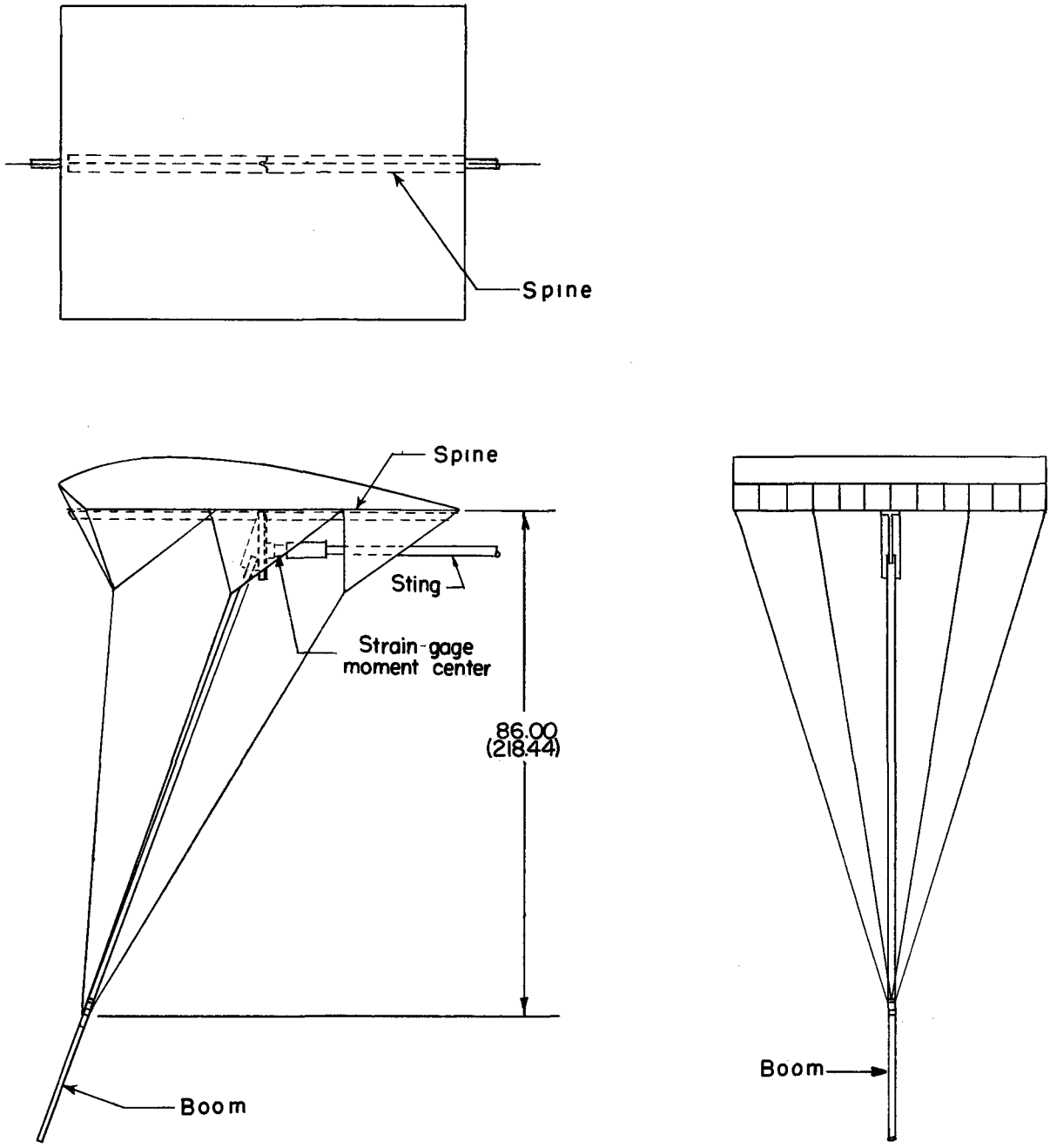

Figure 9.- Sketch of model mounted on test setup 3. Initial dimensions are in inches; parenthetical dimensions are in centimeters. For clarity some hidden lines are omitted in figure.

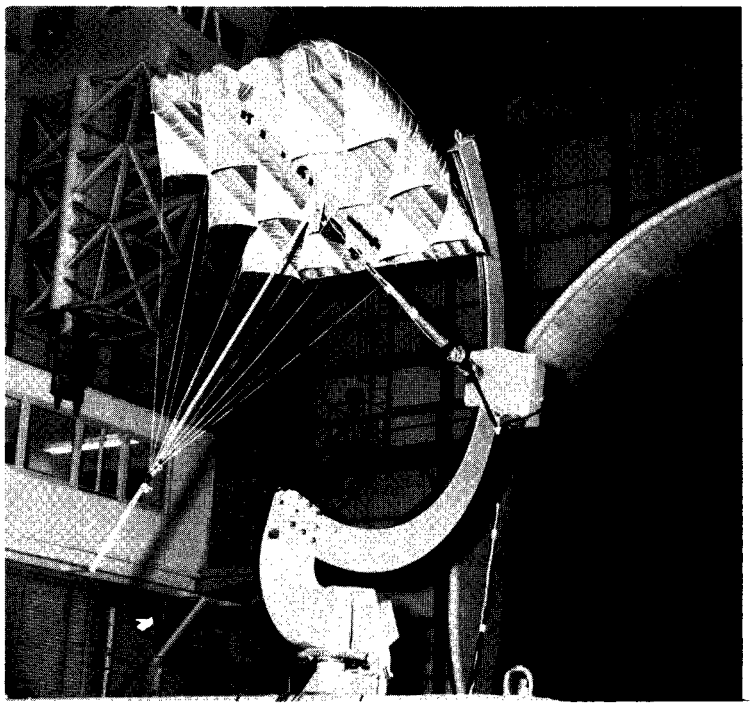

L-65-5437

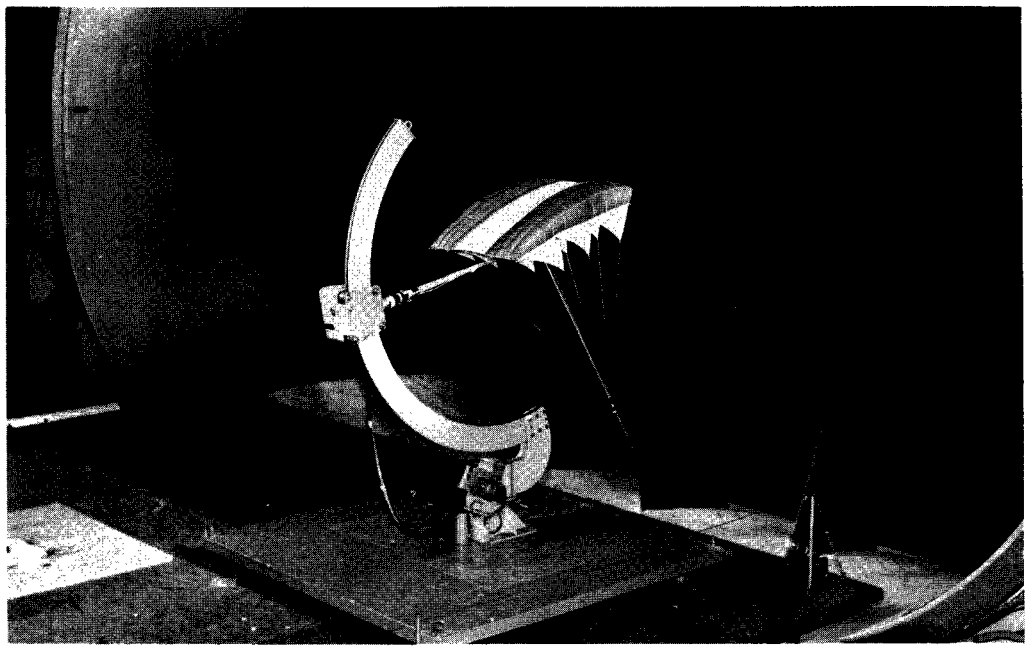

(a) Wing II; test setup 3. L-65-5435

Figure 10.- Wings II and III mounted on test setup 3 in Langley full-scale tunnel.

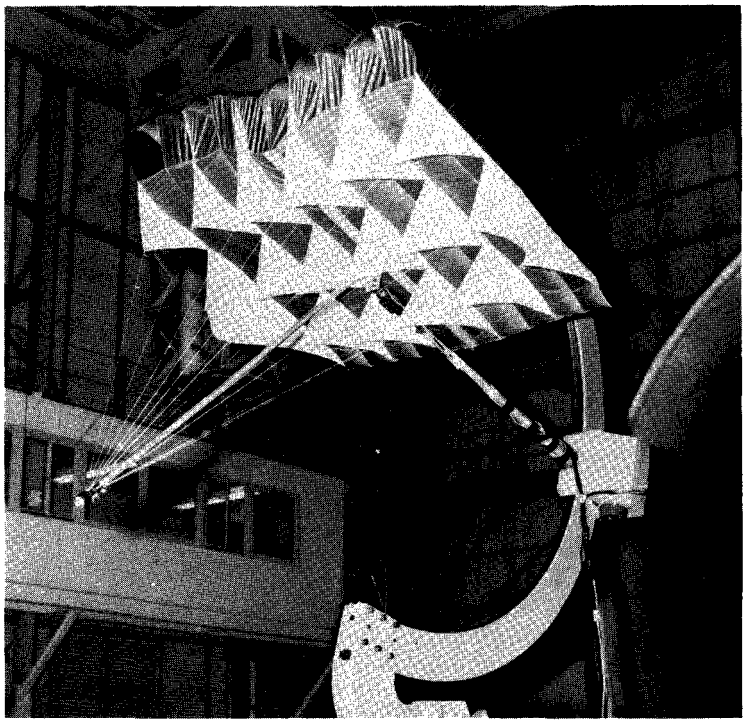

L-65-5683

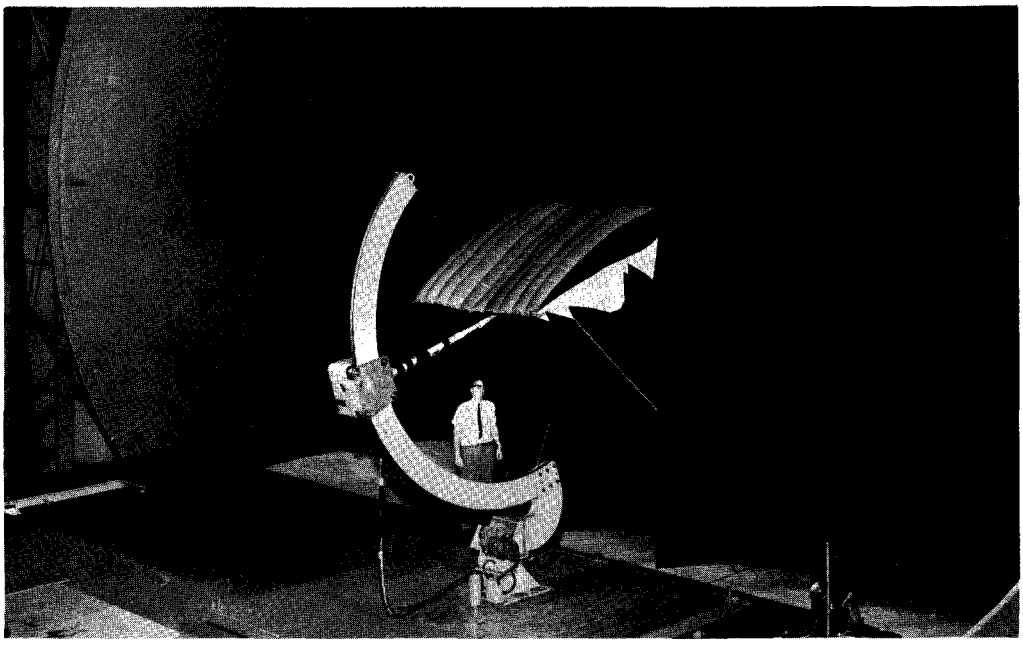

(b) Wing III; test setup 3. L-65-5685

Figure 10.- Concluded.

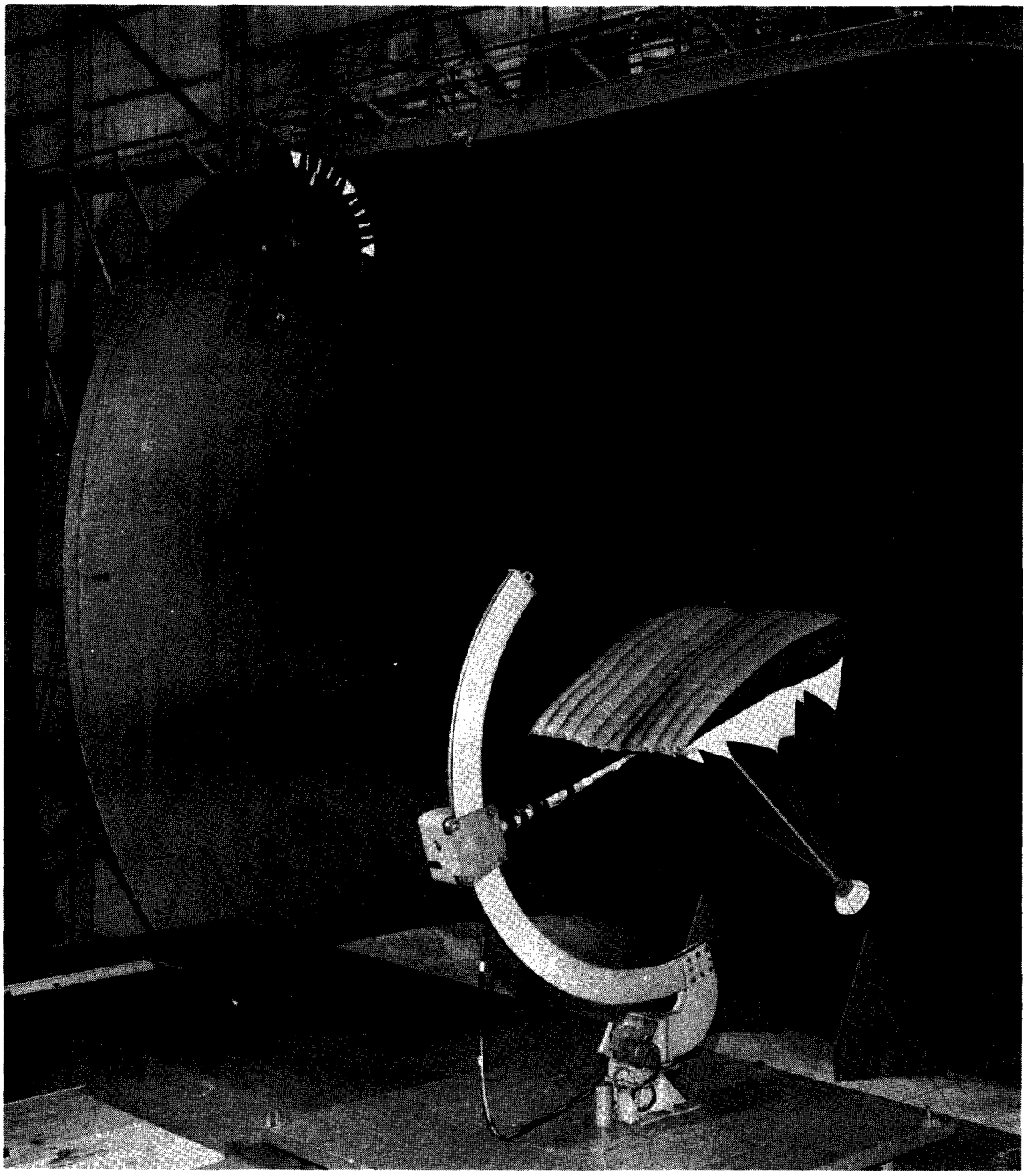

Figure 11.- Wing III with capsule mounted on test setup 3 in Langley full-scale tunnel. L-65-5686

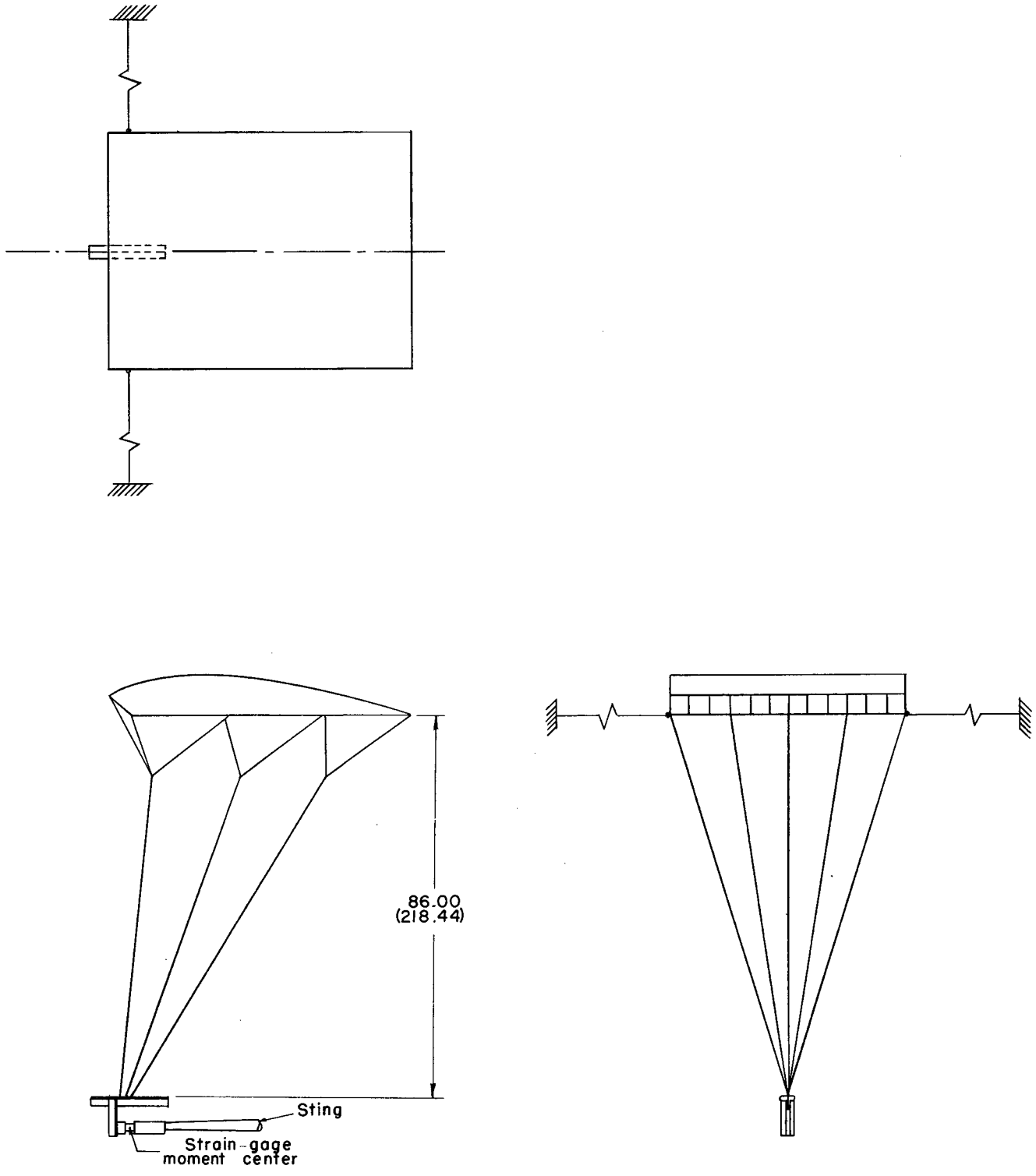

Figure 12.- Sketch of model mounted on test setup 4. Initial dimensions are in inches; parenthetical dimensions are in centimeters. For clarity some hidden lines are omitted in figure.

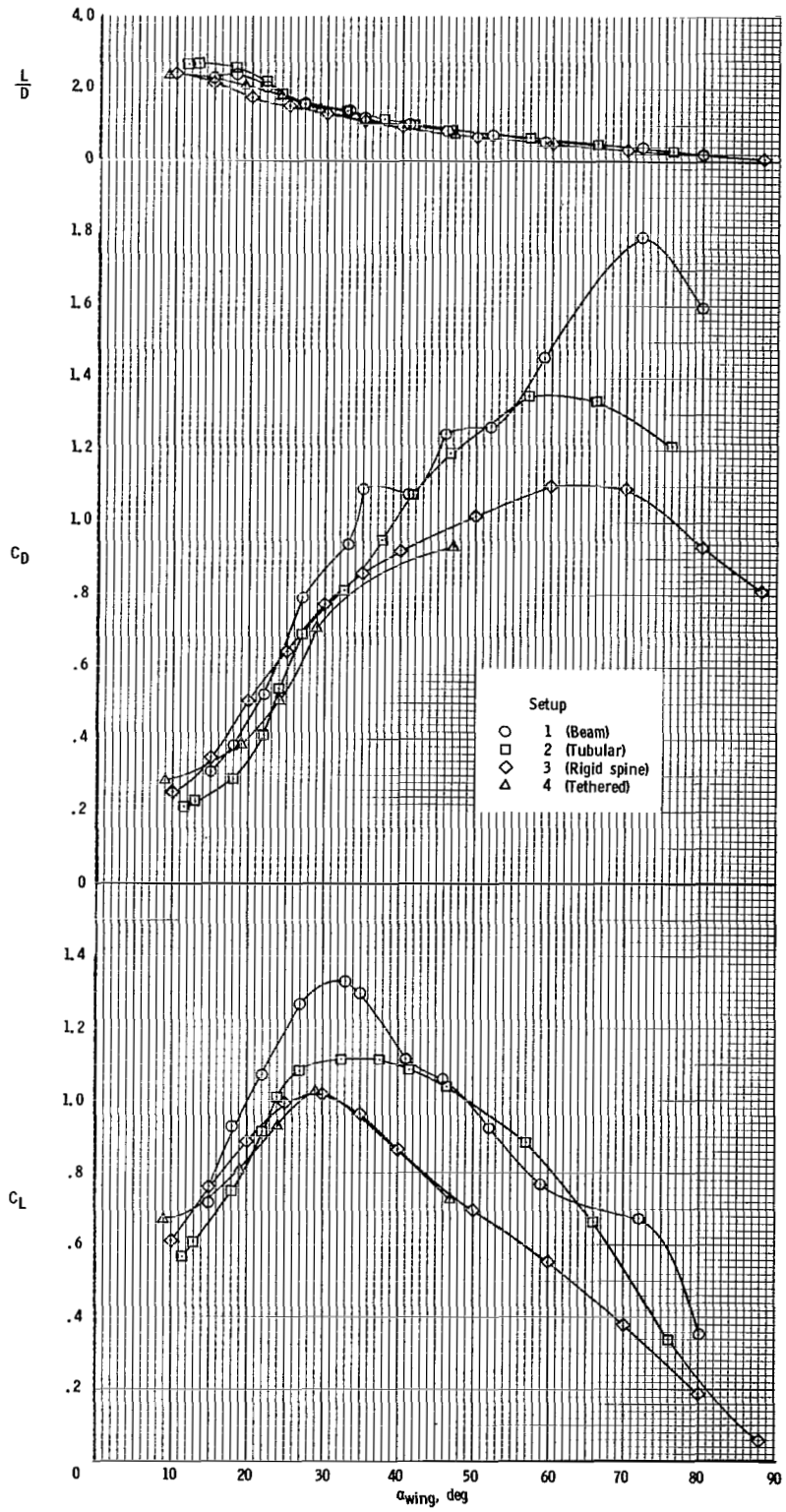

Figure 13.- Effect of test setup on the longitudinal aerodynamic characteristics of wing II. Airspeed, 20 ft/sec (6.1 m/s).

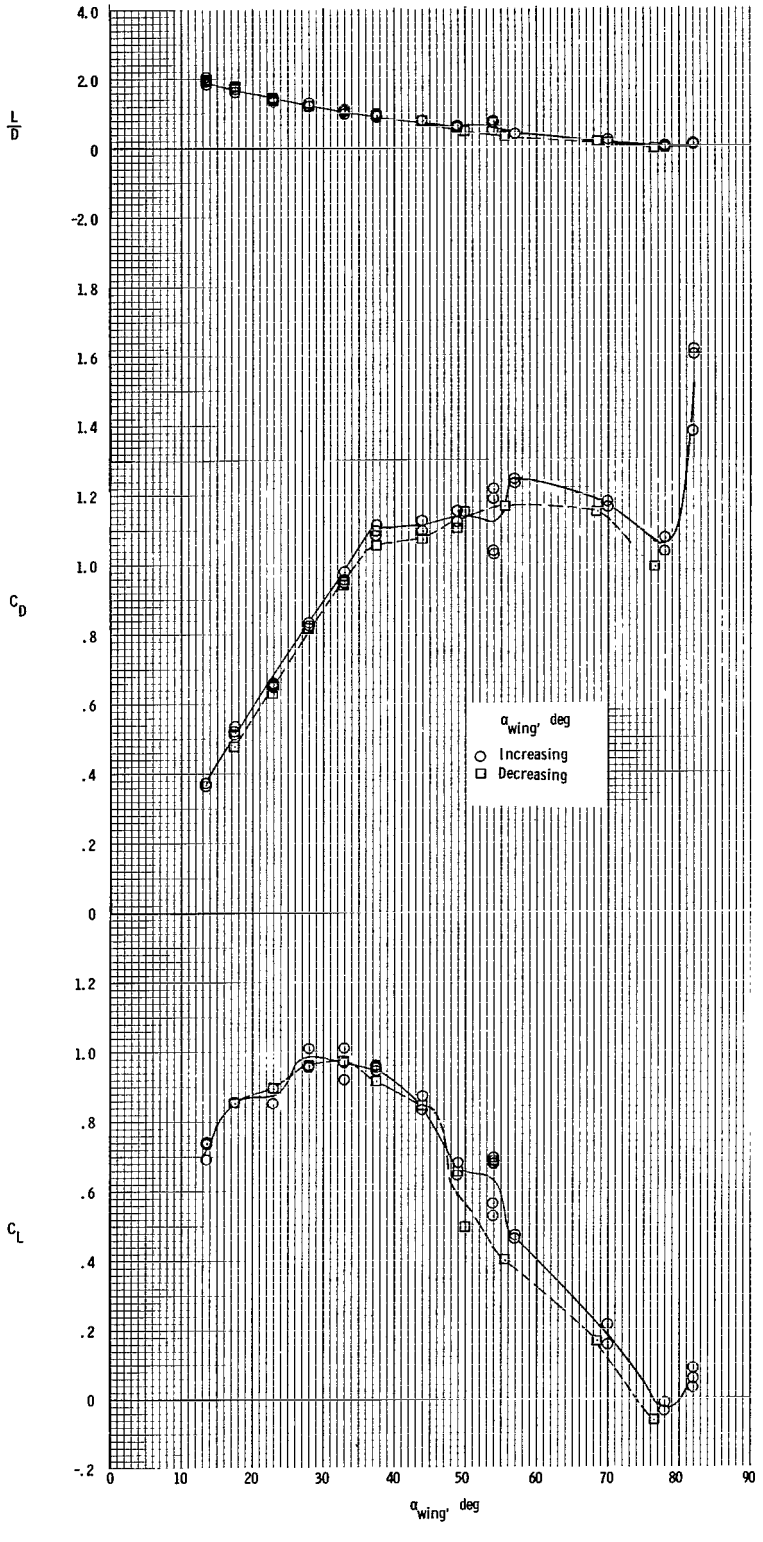

Figure 14.- Longitudinal aerodynamic characteristics of wing 1. Test setup 1.

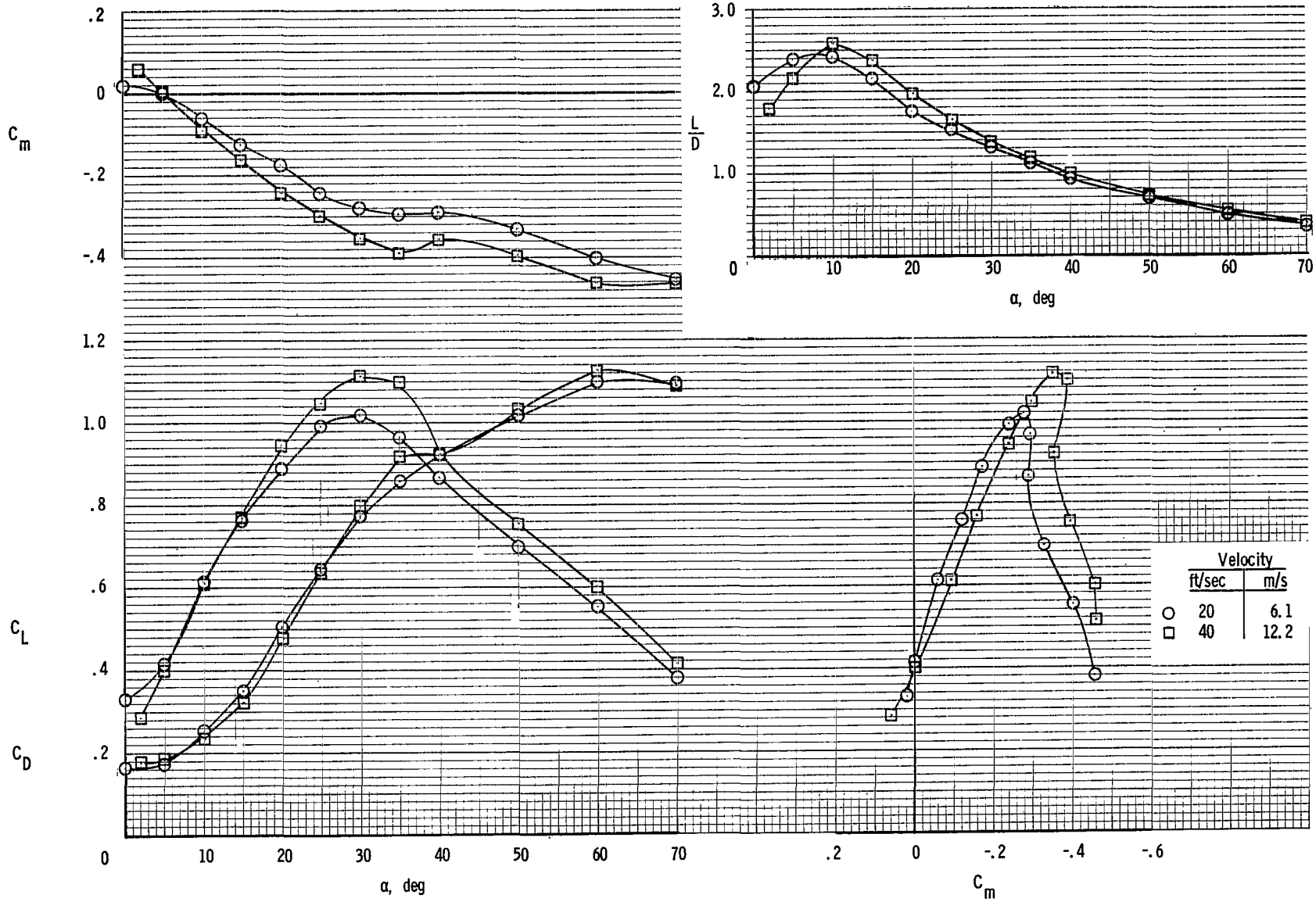

(a) Wing II.

Figure 15.- Longitudinal aerodynamic characteristics of wings II and III. Test setup 3.

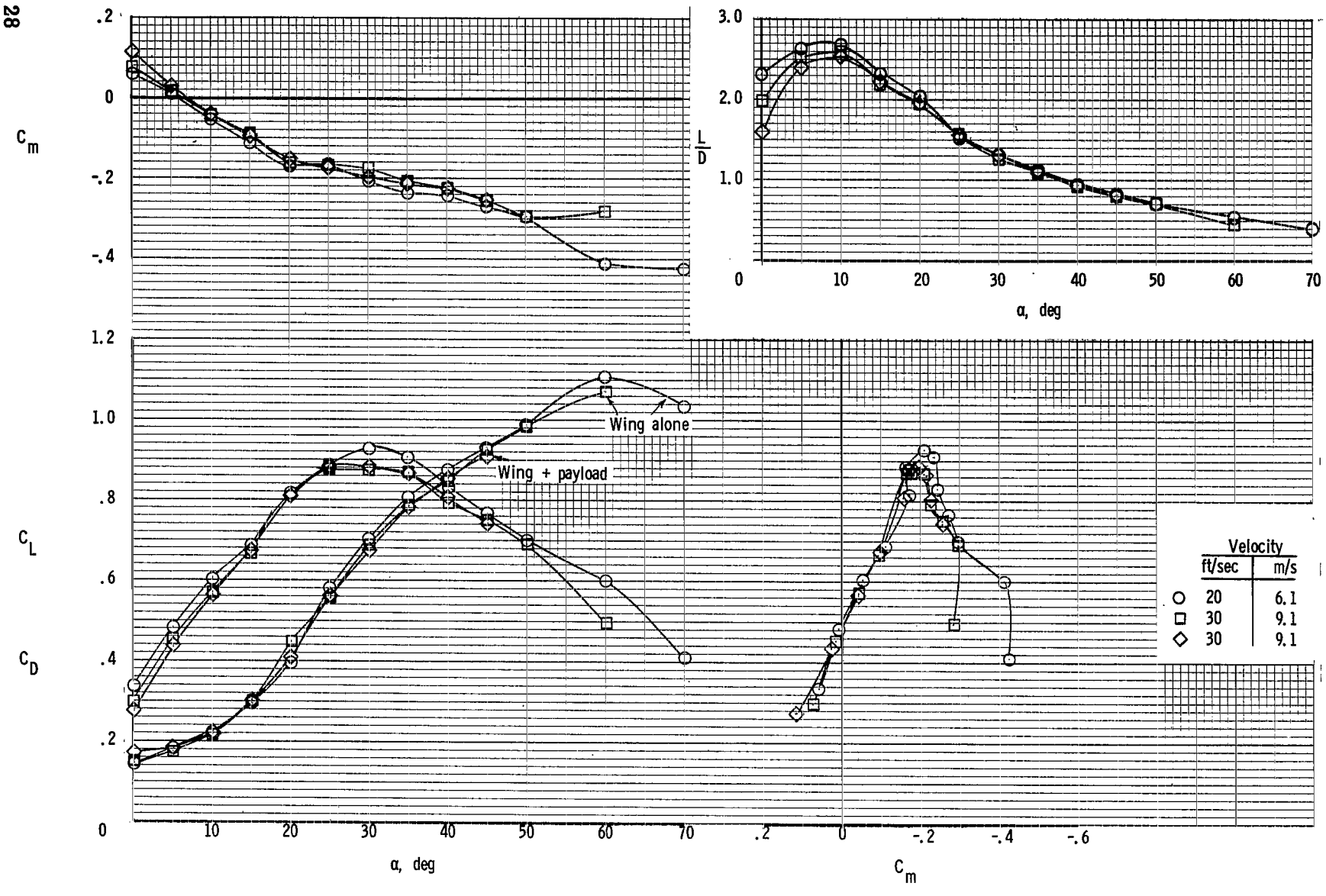

(b) Wing III.

Figure 15.- Concluded.

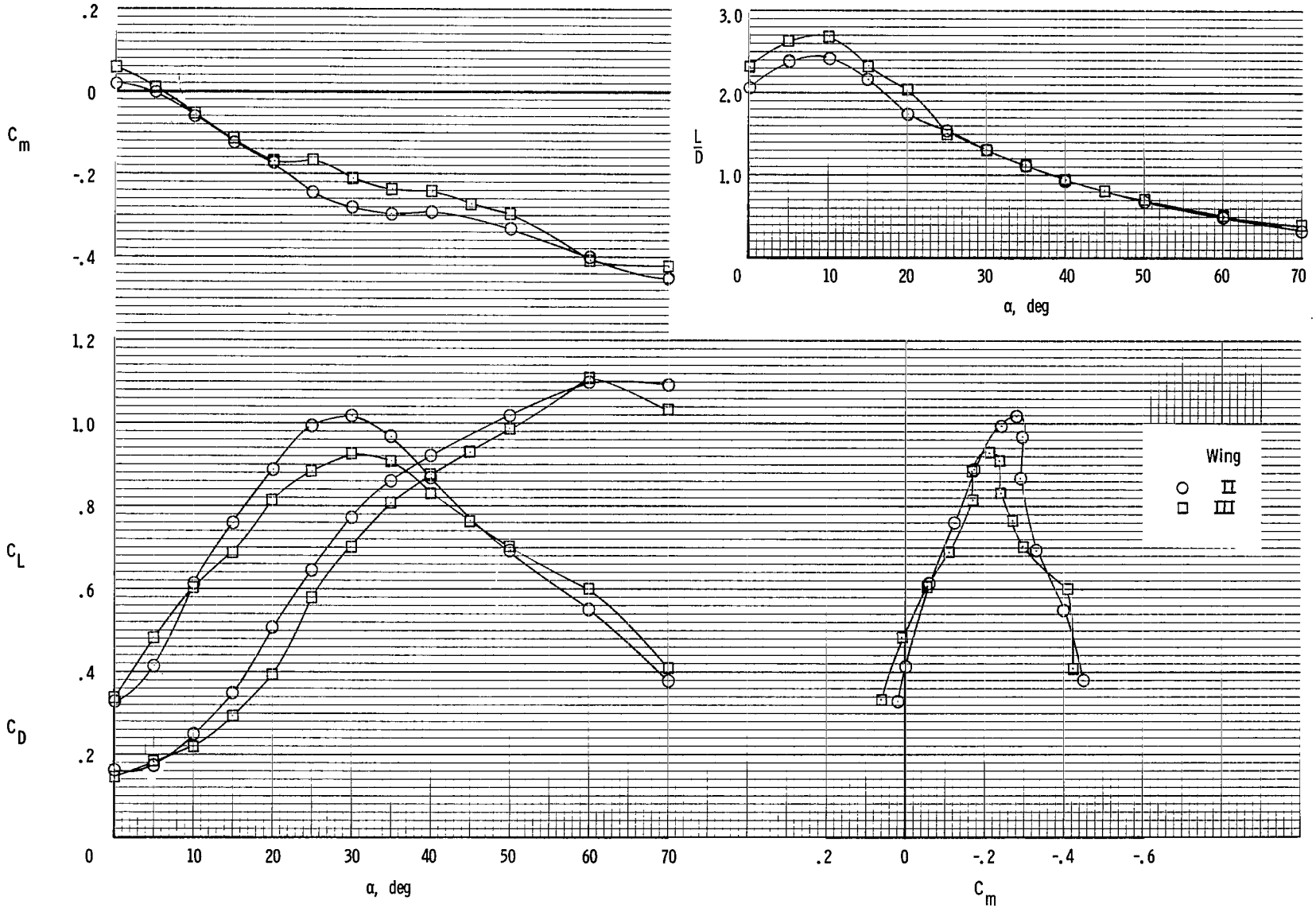

Figure 16.- Comparison of the longitudinal aerodynamic characteristics of wings II and III. Test setup 3. V = 20 ft/sec (6.1 m/s).

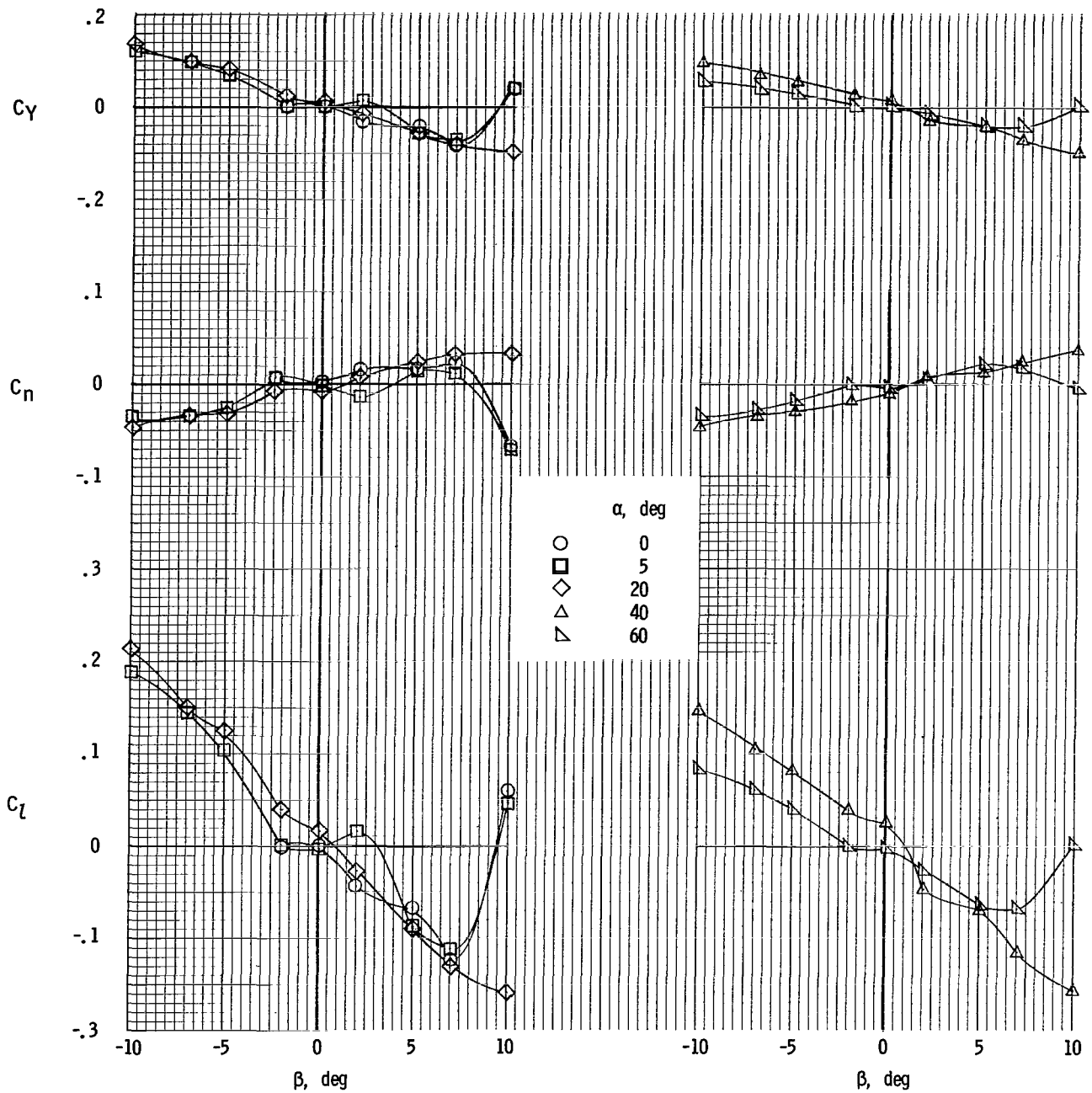

(a) Wing II; V = 20 ft/sec (6.1 m/s).

Figure 17.- Variation of lateral aerodynamic coefficients of wings II and III with angle of sideslip. Test setup 3.

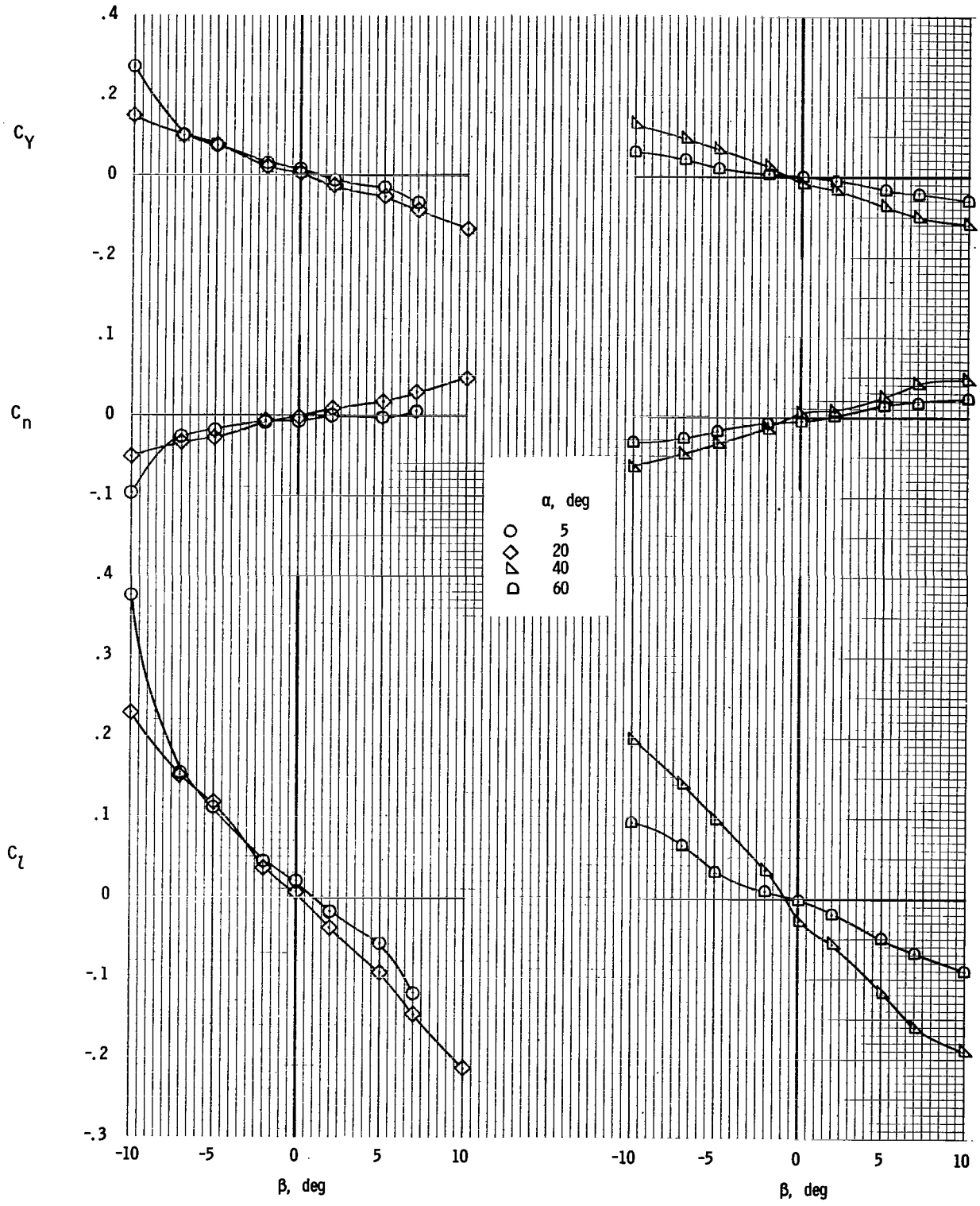

(b) Wing II; V = 40 ft/sec (12.2 m/s).

Figure 17.- Continued.

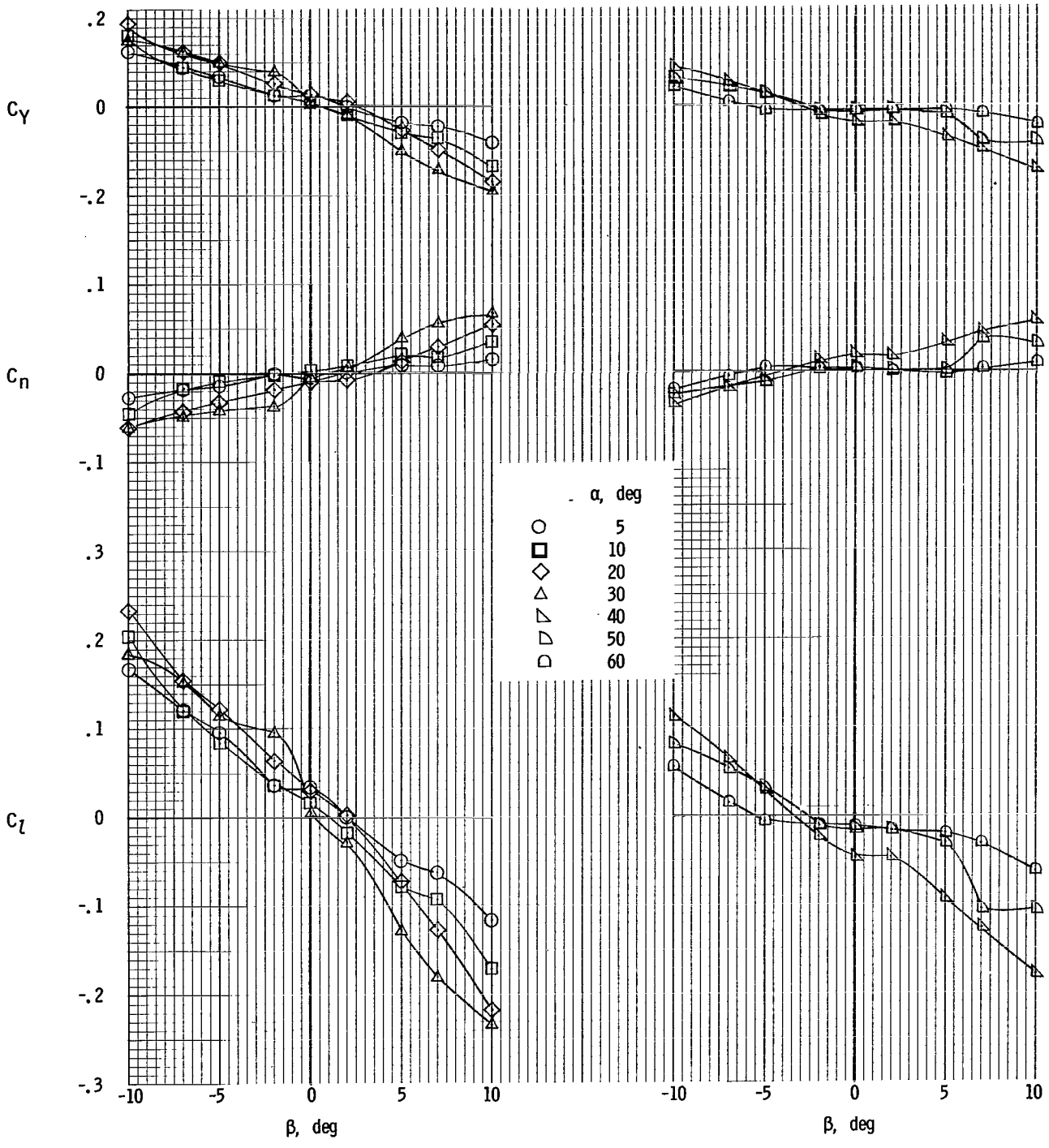

(c) Wing 111; V = 20 ft/sec (6.1 m/s).

Figure 17.- Continued.

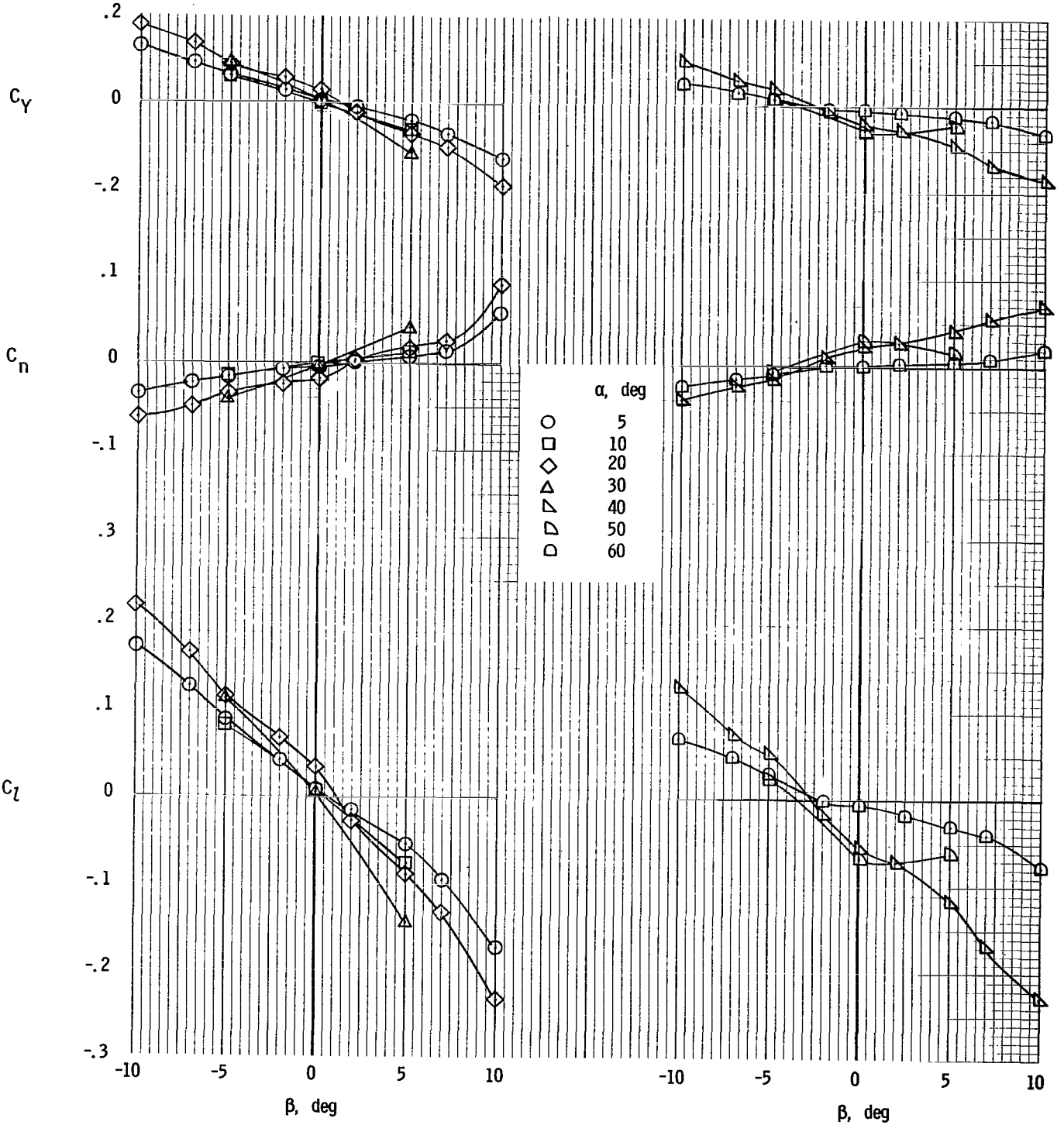

(d) Wing III; V = 30 ft/sec (9.1 m/s).

Figure 17.- Concluded.

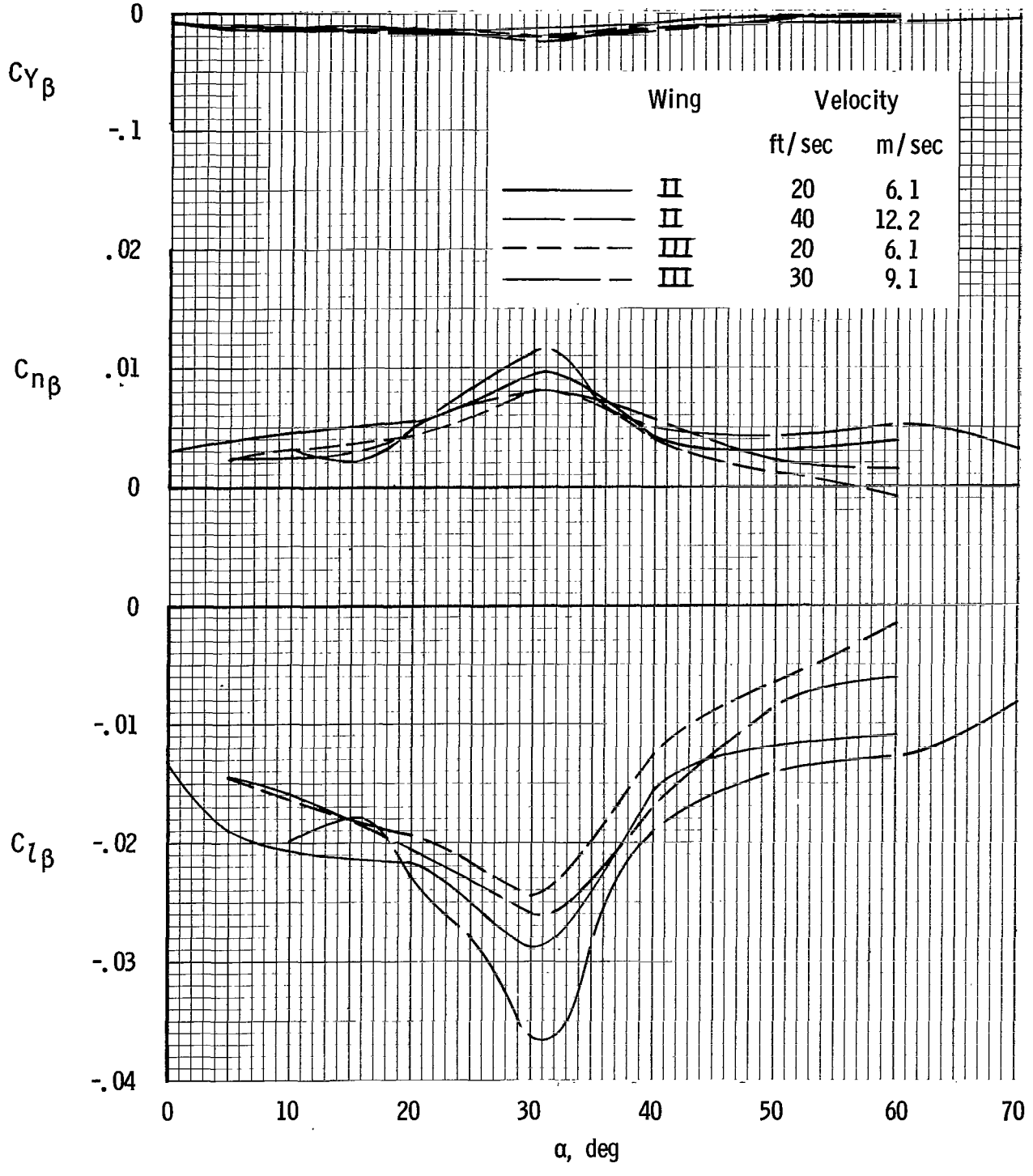

Figure 18.- Comparison of the lateral stability characteristics of wings II and III. Test setup 3.

NASA-Langley, 1967 — 2 L-5765

"The aeronautical and space activities of the United States shall be conducted so as to contribute . . . to the expansion of human knowledge of phenomena in the atmosphere and space. The Administration shall provide for the widest practicable and appropriate dissemination of information concerning its activities and the results thereof."

—NATIONAL AERONAUTICS AND SPACE ACT OF 1958

NASA SCIENTIFIC AND TECHNICAL PUBLICATIONS

TECHNICAL REPORTS: Scientific and technical information considered important, complete, and a lasting contribution to existing knowledge.

TECHNICAL NOTES: Information less broad in scope but nevertheless of importance as a contribution to existing knowledge.

TECHNICAL MEMORANDUMS: Information receiving limited distribution because of preliminary data, security classification, or other reasons.

CONTRACTOR REPORTS: Scientific and technical information generated under a NASA contract or grant and considered an important contribution to existing knowledge.

TECHNICAL TRANSLATIONS: Information published in a foreign language considered to merit NASA distribution in English.

SPECIAL PUBLICATIONS: Information derived from or of value to NASA activities. Publications include conference proceedings, monographs, data compilations, handbooks, sourcebooks, and special bibliographies.

TECHNOLOGY UTILIZATION PUBLICATIONS: Information on technology used by NASA that may be of particular interest in commercial and other non-aerospace applications. Publications include Tech Briefs, Technology Utilization Reports and Notes, and Technology Surveys.

Details on the availability of these publications may be obtained from:

SCIENTIFIC AND TECHNICAL INFORMATION DIVISION

NATIONAL AERONAUTICS AND SPACE ADMINISTRATION

Washington, D.C. 20546